Simulating the Mechanically Induced Response of Energetic Materials

Civil Engineering

Master Thesis

M.P.A. de Jong

TU Delft Delft University of Technology

TNO innovation for life

Simulating the Mechanically Induced Response of Energetic Materials

A Non-Linear Simulation of Finite Element Analysis

by

Miranda de Jong

to obtain the degree of Master of Science
at the Delft University of Technology,
Faculty of Civil Engineering and Geosciences

Student number:	4448669	
Project duration:	November 2020 - April 2022	
Thesis committee:	Prof. dr. ir. L.J. Sluys,	TU Delft (chair)
	Ir. H.P.A. Dijkers,	TNO (daily supervisor)
	Prof. dr. A.E.D.M. van der Heijden,	TU Delft
	Dr. ir. J. Weerheijm	TU Delft

An electronic version of this thesis is available at `http://repository.tudelft.nl/`.

Cover Image: Samantha de Jong

TU Delft Delft University of Technology

TNO innovation for life

Acknowledgements

I want to thank my committee, who, even though it took very long to finish this thesis, were always willing to help. Every meeting gave new insights and every point of criticism was workable and constructive.

I also express my gratitude to my colleagues at TNO who were kind enough to include me in their day to day experience, especially the intervision group with Dieter, Taylor and Wessel. I want to thank Jelme Pennings in particular, who helped with every single LS-DYNA related question I had. Without Jelme, there would not have been a thesis.

I want to thank my parents, Jeroen and Mariëlle, and my sisters, Daniëlle and Samantha. You each helped motivate me and took care of me in your own way. All the pep talks, tea times and thorough reading were very much appreciated. Thanks to Jorn, for everything, but especially for helping me not think about my thesis once in a while. All five of you are invaluable to me.

No one studies alone, so thanks to all my friends. A special thanks to Rens, for every *vragenuurtje* over the years and for being insistent on reading my thesis and weeding out any erroors. Thanks to JC Poolster for showing me the university outside of my own faculty and my friends at CiTG whom I have spent many a day with on puzzling assignments.

Miranda de Jong,
April 2022

Contents

List of Figures

List of Tables

Summary

Munition articles may be sensitive to case-crushing loading. This is a potential safety hazard since it may lead to accidental detonation. A better understanding of the mechanism causing the munition articles to react can help improve safety. A finite element model combined with post-processing is used to model a Steven test. This is a standardised test where a cylindrical steel specimen filled with explosive material is impacted by a steel projectile. The finite element model is then used to identify the most impactful parameters in a parameter study. This thesis specifically looks at the absence or occurrence of a self-sustaining reaction in energetic material PBX-9501, a polymer bonded HMX based explosive. A reference paper (Gruau et al., 2009) was used to model the behaviour and validate some of the results.

The PBX is predicted to react if it has satisfied a certain reaction criterion. The reaction criterion is based on the hot spot theory of ignition. This theory poses that known chemical properties of the material, the plastic shear strain rate and the hydrostatic pressure can predict the occurrence of a reaction.

A finite element model was used to find the plastic strain rate and pressure in the energetic material subjected to a case-crushing loading. Next, the reaction criterion is computed in a separate script. Used programs include LS-DYNA, LS-Prepost and Jupyter notebooks for a post-processing Python script. The finite element model is an axi-symmetric replica of a Steven test as was conducted in the reference paper. The energetic material was modelled as a homogeneous continuum with a Drucker-Prager yield criterion. This material model did not include any post-yielding behaviour, like strain hardening.

First, a finite element model was constructed that was used as the baseline model throughout the thesis. It was subjected to the same loads as a particular Steven test set-up in the reference paper. The combined FEM and post-processing model was shown to be more sensitive than the model in the reference paper. Though the areas with reacted elements roughly corresponded, the model in this thesis had a larger area of reacted elements than the reference paper. The combined model also predicted a reaction at a lower velocity, which, according to real life tests in the reference paper, should have not produced a reaction.

The baseline model, and consequent models, also showed excessive deformation. This can be attributed to the use of a simpler Drucker-Prager material model for the PBX as opposed to the complex material model as used in the reference paper. The plastic yield stress in the energetic material was quickly reached and adding strain hardening behaviour would have mitigated the excessive deformation. The absence of any hardening behaviour, and the resulting deformation, also contributed to the instability of the finite element model.

A parameter study was conducted by adapting the baseline model. Varying the velocity of the projectile was the most impactful change. Increasing the thickness of the cover plate was also highly effective in reducing the number of elements satisfying the reaction criterion. Changing properties of the energetic material was not as effective. The change in the compressive strength of the PBX needed to be relatively large to get the same decrease in the number of reacted elements.

In conclusion: the developed model gives a first indication of parameters that contribute to the sensitivity of certain munition articles to case crushing. However, the material model used should be improved to create a more stable finite element model. An improved material model could also better capture the mechanical behaviour of the complex energetic material. It is recommended that future research should focus on this improvement. Improving the predictions in an axi-symmetrical setting for a controlled test specimen could eventually lead to full 3D analyses on realistic munition articles with predictive value.

1 Introduction

Due to the dangerous nature of munition articles, it is of the utmost importance that stringent safety standards apply when working with them. However, accidents could still occur, and knowledge of the causes, consequences and of the likelihood of accidents can be used to improve overall safety.

Munition articles can be stored in storage magazines. One of the hazards in storage magazines is a sympathetic detonation. This means that a munition article iss not supposed to detonate or deflagrate, but does so anyway, usually caused by another explosion. In order to prevent sympathetic detonations, a storage facility is designed with safety measures. These include prescribed distances between different magazines and other facilities (QDs) or that different types of munition articles are separated from each other (North Atlantic Treaty Organization, 2015). This thesis focuses on a sympathetic detonation that is caused by one specific hazard: spall.

Figure 1: Heavy spalling as encountered in a field experiment by TNO. The blast came from the right side of the figure. (Wees et al., 2007)

1.1 An Introduction to Spall

The focus of this thesis is on a scenario involving spall, see Figure 1. A munition article might detonate due to direct shock, case crushing, fragment impact and subsequent penetration, or thermal cook-off (Cooper and Kurowski, 1996). Spall can potentially cause a case crushing type of loading. Spall is the ejection of debris pieces from a structural element, in this context, due to an explosion. The debris is formed due to air blasts or impact from other debris on the structural element. This means that spall can occur in a munition magazine adjacent to an exploded magazine, if the distances are small enough.

Scientifically speaking, spall 'occurs when two strong plane decompression waves under uniaxial strain conditions interact to produce a region of tension in the interior of a material body' (Antoun et al., 2003), which is similarly phrased in *Introduction to the Technology of Explosives* (Cooper and Kurowski, 1996). In simple terms: stress waves interact in the material creating tensile stresses that pull apart the material. Certain structural elements, like concrete walls, are particularly weak to tension and are easily damaged by these stress waves. In the context of a munition storage magazine, spall can occur when a (large) explosion occurs in an adjacent magazine. The shock wave from this explosion will travel to the walls of neighbouring magazines. When this wave is reflected within the walls, it creates a tension wave. The wall fails under the tension on the non-loaded side. This launches debris pieces into the magazine. Bear in mind that this is a very theoretical definition, and not all types of spall are included in this definition.

This thesis will therefore refer to spall as *the loosening of pieces of debris from walls, roofs or other structural elements due to a nearby explosion.* In this way, also non-shock induced spall will be included. This broader definition is desirable because this thesis is concerned with the phenomena occurring in the crushing of a munition article as might be caused by spall. Further research into the nature of spall is not

included in the scope of this thesis.

Some explosives or ammunitions are more sensitive to spall than others. NATO publications prescribe different sets of storage rules for ammunition that is vulnerable to 'heavy spalling'(North Atlantic Treaty Organization, 2015). Munition articles are subdivided into sensitivity groups that have different reactions to varying types of loads. These sensitivity groups then determine the way in which way these munition articles can be safely stored and what limitations apply to the storage. At the present time, there are five different Sensitivity Groups (SG). Only SG5 contains ammunition articles that are sensitive to spall (North Atlantic Treaty Organization, 2015). Not every munition article within that group will react the same to a similar load. When the different types of munition articles can be modelled more precisely, the real sensitivity of the munition articles, and the difference between the different munition articles within certain Sensitivity Groups, can be estimated more precisely.

1.2 Scenario and Approach

Imagine a storage magazine filled with ammunition articles that are sensitive to a crushing type load that can lead to unintended initiation of those articles.: magazine A. This particular magazine is situated next to another storage magazines. An accident occurs in a neighbouring magazine B, causing a large explosion. Magazine A is hit by debris and will be hit with a sizeable air blast. The load causes one of the concrete walls of the magazine to collapse. The resulting debris will be propelled through the area with considerable speeds and large masses, quickly impacting an unprotected sensitive munition article. How will this munition article react?

This thesis aims to provide a method to find which mechanical parameters cause munition articles to be more sensitive to a crushing type loading. Whether a reaction occurs is quantified in a reaction criterion: a calculated value that should indicate whether a part of the energetic material will or will not react. With a reaction, any type of explosion reaction ((partial)detonation, deflagration, or burning) is included. This thesis serves as a first research: the methodology discussed can be expanded upon later.

1.2.1 Research Question

The main research question is:

Which parameters are dominant in preventing a reaction in a munition article subjected to a crushing type loading?

To answer this question and break it down into more manageable pieces, the following sub-questions are asked and answered:

- Which simplifications can be made to create a model?
- Which loading parameters on the munition article are the most critical in preventing or allowing a reaction?
- Which munition article properties are the most critical?

1.2.2 Scope

A clear scope was defined for this thesis. Below is a list with boundaries and assumptions, that will be explained within the thesis.

This scope of this thesis ***includes***:

- Non-linear material behaviour
- Time-dependent explicit finite element analysis
- Only one type of energetic material (PBX-9501)

This thesis ***excludes***:

- The behaviour of the energetic material after initiation
  - The severity of the reaction of the energetic material
  - Deformations caused by a reaction in the energetic material
- Micro-scale modelling

The following ***assumptions*** are included in the scope, see Section 2:

- The energetic material can be modelled homogeneously
- Continuum finite elements will be used

1.3 Structure of this Thesis

This thesis aims to document the process of building a non-linear finite element model to predict the occurrence of a reaction in a munition article due to a crushing type loading. First, the energetic material inside the munition article is discussed. This includes its properties, reaction circumstances and how a reaction criterion can be modelled using numerical approaches in a script, see Figure 2.

Second, a detailed explanation of the baseline model is given. This model will sever as the basis for parameter studies and is a first look at the feasibility if the method. The model is compared to tests and a reference paper, as a check to see whether the outcomes from the model are realistic. The accuracy of the model is checked and deviations from the practical tests are discussed.

This is followed by a parameter study to find the variables that have the most impact on the phenomena. Different properties of the baseline model are varied to gain more insight into the phenomena related to mechanically induced reactions.

Finally the conclusion and discussion will provide an overview of the research, its successes and its recommendations for improvements in future research.

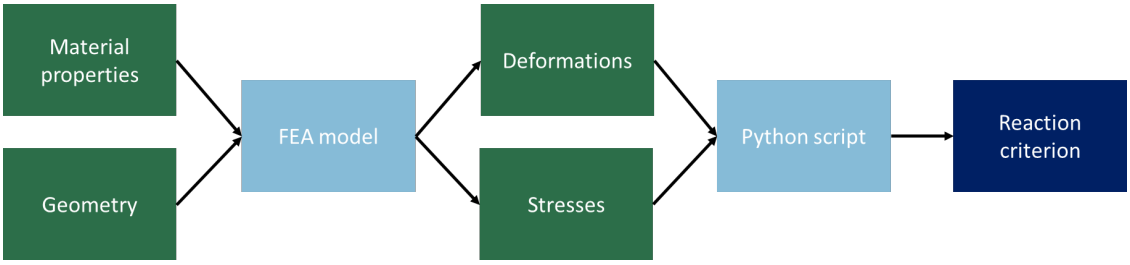

Figure 2: Steps involved in computing the reaction criterion.

2 Simulating the Energetic Material

The energetic material is modelled in order to gain an understanding of the mechanical response of energetic materials due to a low velocity (< 100 m/s) impact loading. This section will explain some properties of energetic materials. It will explain the theory behind the reaction criterion and how this material is modelled in a finite element analysis. Next, the implementation of the reaction criterion in a script is discussed. This is referred to as the post-processing phase.

2.1 Physical Properties of the Energetic Material

This thesis will look at a plastic bonded explosive (PBX), specifically PBX-9501. PBX's consist of HMX particles mixed with a polymeric binder (Cooper and Kurowski, 1996). This means that the material is heterogeneous. Its properties depend on the properties of the binder and the granules and on their proportion in the mixture. This makes modelling the behaviour of the material more complex.

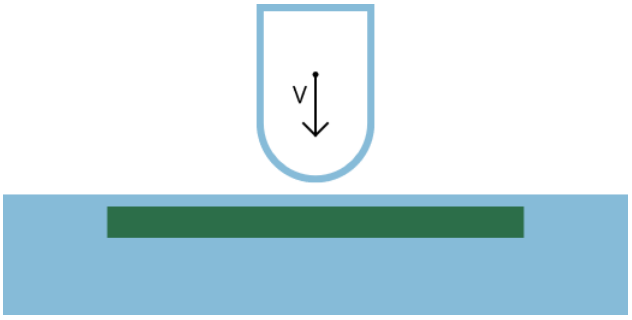

Figure 3: Cross-section of a Steven Test. A projectile (light blue) is fired at a steel target (light blue) with velocity v. The target envelops the energetic material (green).

2.1.1 Occurrence of Reactions in Energetic Materials

Some energetic materials are sensitive to fast deformations and will be more likely to react to a low velocity impact loading. This behaviour is usually found using tests such as the Susan (Cooper and Kurowski, 1996) or Steven test (Chidester et al., 1993), see also Figure 3. Both tests consist of a projectile that is fired towards a target: in a Susan test the energetic material is encased in the projectile, whereas a Steven test has the energetic material inside a target plate. The velocity of the projectile and the reaction of the energetic material are logged and can be used to compare the sensitivity of different materials. TNO has also conducted tests similar to the Steven test, that showed that the speed of a projectile plays an important role in the severity of the reaction (Scholtes and Verbeek, 2010).

Researchers can also perform numerical analyses to predict whether an energetic material reacts. However, these still need to be validated with physical tests. Therefore, many researchers choose to use physical tests, usually the aforementioned Steven test, to test the validity of their models. (Gruau et al., 2009; Picart et al., 2013; Lou et al., 2017; Liu and Chen, 2018).

2.1.2 Mechanical Properties of Energetic Materials

Generally speaking, the properties of energetic materials are hard to come by. Due to the applications of explosive materials, interested parties may want to keep their knowledge to themselves for security reasons. On top of that the material is difficult to test due to its violent and complex nature (e.g. its non-homegeneity) (Manner et al., 2017). Though practical tests are still conducted (Ellis et al., 2005; Scholtes and Verbeek, 2010).

As an alternative to field tests, it is possible to use a different material that has similar mechanical properties and a similar composition as energetic materials. For example: Ravindran et al. (2016) used sugar and a binder as a substitute for HMX crystals and its matrix. These studies can be used to find relations between stresses and strains in complex materials and facilitate modelling of these materials. This

type of research is conducted to gain more insight into the properties of the material under different loading conditions. The research can be used to estimate mechanical properties in a safer way and make numerical models more accurate. However, substitute materials are never fully representative of the energetic materials.

2.1.3 Mechanical Properties in this Thesis

Since little is known about the mechanical behaviour of PBX's in general, only one type of PBX is considered in this thesis. This is PBX-9501 as used in the reference paper for the reaction criterion (Gruau et al., 2009) that will be discussed in Section 3.5. The tests from this paper can be used to compare the results from the approach of this thesis to the results of the paper itself. Theoretically, the reaction criterion used can be applied to a wide range of PBX's, but certain parameters will need to be calibrated using tests. The method can also be applied to other similar energetic materials, but tests alongside specific material properties will be needed to calibrate the model.

This thesis models the material as a homogeneous material with isotropic properties. This is the same assumption as is taken in the reference paper(Gruau et al., 2009). The assumption that PBX's are homogeneous significantly simplifies the analysis, which is acceptable in a first model. The assumption can be made because the micro-level contact between the granules is already modelled in the chemical model (Browning and Scammon, 1995; Browning, 2002). This means that this level of material behaviour is not necessary for the computation of the reaction criterion.

2.2 Reaction Criterion

The reaction is caused by a type of mechanical initiation (Cooper and Kurowski, 1996), as discussed in Section 1. A reaction occurs when the reaction criterion in an element has reached a certain threshold value. The theory chosen to model this behaviour can be found in the reference paper (Gruau et al., 2009), which is in itself a modified version of works from (Browning and Scammon, 1995; Browning, 2002). This method is based on the relative sliding of HMX granules at a micro-level. The total produced energy flux is then taken over a volume. The behaviour of the HMX-granules is scaled up to be understood in the context of meso-scale parameters. Relevant parameters include, but are not limited to the pressure, the granule size and the amount of deformation.

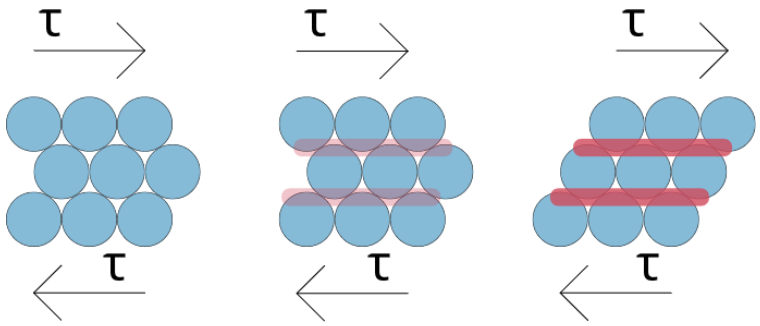

Figure 4: Visualisation of shear strain causing plastic shear strain and its associated heating at contact points (red). Note: this is a simplification, the matrix binder is excluded and HMX granules are not necessarily arranged in such a pattern. Based on Figure 9 in Gruau et al. (2009).

2.2.1 Hot Spot Theory of Ignition

Mechanical initiation in PBX's is based on the hot spot theory of ignition (Cooper and Kurowski, 1996). The energy flux that will lead to a reaction in the material is caused by intergranular sliding friction, see Figure 4. The basis of the reaction criterion is that heat is generated during plastic shear deformation in the material, but only when this occurs under pressure (Browning, 2002). This heat is generated very locally, and is referred to as a hot spot. The generated heat can be enough to cross the threshold of the activation energy of the energetic material, producing a reaction in one of the molecules (Bowden and Yoffe, 1985).

A hot spot that can lead to a self-sustaining reaction is called a critical hot spot (Field, 1992; Handley, 2012). A critical hot spot will cause a detonation/deflagration, since it produces enough energy during its reaction in order for the reaction to propagate through the material. A sub-critical hot spot, i.e. a hot spot that is not large or hot enough, will not generate a reaction. The size of the critical hot spot varies per material and temperature of the hot spot but the size of the hot spot is generally between 0.1 and 10 μm (Bowden and Yoffe, 1985).

When the material is subjected to a shear stress, see Figure 4, the individual HMX granules captured in the binder will be forced to slide over each other. The resulting friction forces generate heat and when enough force is exerted on the particles they will move to their new position in a plastic deformation.When this process takes place under pressure, the forces between the granules are larger, leading to more friction and thus more heat generation (Gruau et al., 2009). This friction can also be generated along the microcracks in the material (Barua and Zhou, 2011; Liu and Chen, 2018).

The models presented in Browning and Scammon (1995); Browning (2002) do not take the friction due to imperfections like microcracks into account. Here, the contact area of the particles is only based on the Hertz contact stress and a modelled latticework of particles. See also the section 'Coupling macroscopic state to microscopic state' in Browning (2002). The local frictions lead to a heat flux that causes chemical decomposition of the energetic material. Given enough chemical decomposition of the material, a self-sustaining reaction can be reached. This will count as a reaction in this thesis, as Browning (2002) refers to the relations as 'an ignition criterion'.

2.2.2 The Initiation Mechanism

Most of the work of this part of the thesis is based on equation 1 as taken from Gruau et al. (2009). This particular equation contains the necessary information to determine whether or not the munition article will react due to the deformation. The different variables are explained below.

To simplify and summarise the equations: under enough pressure and with enough deformation for a set amount of time, the reaction criterion in a single element will be satisfied and a reaction will occur. See also equation 1. Variables and a short explanation can be found below.

$$\frac{1}{c*}\int_0^{t_{ig}} \frac{(t_{ig}-\tau)^{-n}}{t*}\left(\frac{\langle p(\tau)\rangle}{p*}\right)^{2n/3}\dot{\bar{\gamma}}_{pl}(\tau)d\tau = 1 \tag{1}$$

- c* = 4.867e4 (Gruau et al., 2009). c* is a measure of the amount of energy needed for a single element to fulfil the reaction criterion. c* is a value that is calibrated with tests.
- t_{ig} [s] is the time to ignition. This indicates that the reaction is fulfilled when the integral has been taken from 0 to t_{ig}.
- τ [s] is used to denote time, so as to not be confused with t_{ig}.
- t* is the characteristic time equal to 1 s. It is included to eliminate any units in the equation and ensure the equation is equal to a unitless 1. It does not have any physical significance, it is only included to simplify the equation.
- $\langle p(\tau)\rangle$ [Pa] is the positive hydrostatic pressure. The pressure is a function of time and is one of the variables that can be found using the finite element model.
- p* [Pa] is the characteristic pressure equal to 1 Pa. It is included to eliminate any units in the equation and ensure the equation is equal to a unitless 1. It does not have any physical significance, it is only included to simplify the equation.
- n [-] is an exponent that is related to the chemical decomposition of the material. This is a value specific to the energetic material. The value is fitted on the relations 'between the ignition time t_{ig} and a constant (heat) flux ϕ', see also Appendix 2 in Browning (2002). Throughout this thesis $n = 0.447$ will be used, since the exact same PBX is used as in Gruau et al. (2009).

- $\dot{\bar{\gamma}}_{pl}(\tau)$ $[s^{-1}]$ is the plastic shear strain rate. This plastic shear strain rate is a function of time and is one of the variables that can be found using the finite element model.

It is important to note that the used c* is an average of the lower and upper bounds of Gruau et al. (2009). These bound were empirically determined using tests and might contain inaccuracies. The same value from Gruau et al. (2009): c* = 4.867e4 is used in this thesis. When applying equation 1 to a different material than PBX-9501, this value has to be recalibrated by conducting new tests. Exponent n has to be changed too, since it is a constant determined by the type of energetic material.

2.3 Simulation in a Finite Element Program

Finite element codes can be used to compute and visualise a myriad of responses to different types of loading on many materials. This thesis is mainly concerned with the accurate portrayal of impact loading, stress and strain distributions and visualising these aspects. LS-DYNA (version smp d R11.1.0) combined with LS-PrePost (version 4.8) were used in all simulations.

2.3.1 Finite Element Method to Simulate the Situation

The Finite Element Method (FEM) is a numerical method to find the mechanical response of materials to a variety of loading conditions. FEM can be used to run costly experiments with energetic materials in safer and cheaper way. FEM has to potential to contribute much to this scientific field, if the coupling of the mechanical and chemical properties can be linked.

In the case of this thesis, the specific loading conditions on the munition article or test set-up like weight, size or velocity of the projectile or specimen can be changed relatively easily. Since an aim of this thesis is finding the important parameters in the reaction of a munition article to spall, it is a relatively fast way to change the 'set-up' of the experiment.

Using a model instead of doing real-life tests always leads to simplifications that might influence the result. The model can be made with much more detail, but that will cost time, in labour and computational time, and also needs reliably data on the extra details. Since this thesis is a starting point, some simplifying assumptions are made, as discussed in Section 1.

2.3.2 Notes on Scale and Hot Spots

The scale of hot spots as discussed in Section 2.2.1,somewhere between 0.1 and 10 μm, is very small. These hot spots are too small to model as a single element. The final mesh size in the finite element model is 0.5 mm, see Section 3.3. So each element can potentially contain multiple hot spots. This thesis will not scale down the mesh size to only encompass a single hot spot, but will instead have the mesh size depend on the demands from the FEM.

This choice is made for two reasons. Firstly, because the energetic material is assumed to be homogeneous and a continuum in the scope of this thesis. This is based on the theoretical model from Browning (2002); Browning and Scammon (1995), where the reaction criterion is calculated over a volume of the material, not a single hot spot of 0.1 to 10 μm. In this thesis, this volume corresponds to a single element. Since this chemical model is used, it is not necessary to make a smaller mesh.

Secondly, modelling the energetic material would be significantly more demanding computationally. The computation time would be vastly higher and the model would not give significantly extra insight into the mechanical causes for the hot spots. Since this last part is the focus of this thesis, it is not necessary to make a mesh that small.

2.4 Implementing the Reaction Criterion

The formula for the reaction criterion (as discussed in 2.2) should be coupled to the data from the Finite Element Analysis. A separate Python script is used to compute the reaction criterion for each element over time, since implementing this criterion in LS-DYNA is too complex. For a visual explanation of the Python script, see the flowchart in Figure 5. The Python script is conceptually described in the flowchart, for the full script, including some notes, see Appendix A. Some elaboration on the numerical methods is discussed below.

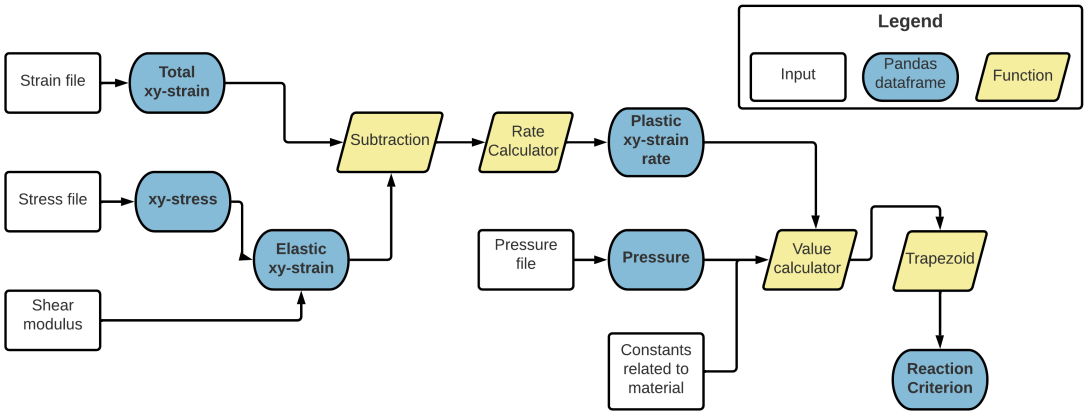

Figure 5: Flowchart of the Python script. The names of the functions are the same as used in the Python script, see Appendix A. The pressure can be taken directly from the output of the finite element analysis. The plastic shear strain rate has to be determined with multiple quantities. See also equation 1 for the necessary variables.

2.4.1 Converting LS-DYNA Output to Input for the Reaction Criterion

The plastic shear strain rate, the pressure and chemical material qualities are needed to compute the reaction criterion. LS-DYNA directly generates the pressure from the finite element analysis. This pressure data is then converted to a DataFrame in the Python script, see Figure 5.

The plastic shear strain rate is not an automatic output of LS-DYNA. So, this is calculated in the post-processing phase. The total xy-strain is available, but contains both the plastic and elastic part. The elastic part can be calculated, by taking the xy-stress and dividing by the shear modulus of the material, see equation 2. The relationship between the elastic shear stress τ and the elastic shear strain γ_e is linear. When both the total shear strain and the elastic shear strain are known, a function is used to subtract them from one another. This gives just the plastic shear strain, see equation 3.

$$G * \gamma_e = \tau_e \tag{2}$$

$$\gamma_{total} = \gamma_e + \gamma_{pl} \tag{3}$$

The next step is converting the plastic shear strain to a plastic shear strain rate. This is done using a numerical derivative: $\dot{x} \approx \Delta x / \Delta t$. Where Δx is the difference in the plastic shear strain rate from time t_1 to t_2 and Δt is the same fixed time step as used in the finite element analysis.

2.4.2 Evaluating the Integral

LS-DYNA, the used finite element program, produces a discrete output. This means that evaluating the integral in an exact manner is impossible, since for instance, the values for p and $\langle\tau\rangle$ are only known at set times. The Trapezoidal Rule (Stewart, 2012), see equation 4, is used to evaluate the integral. This numerical method was chosen because it gives an output on the points in time where data is available, not averaging in between two data points. Due to the high forces in the energetic material at time of impact causing division by 0, the contribution to the integral is manually set to 0 at time of impact. See also Appendix A.

$$\int f(x)dx \approx T_n = \frac{\Delta x}{2}[f(x_0) + 2f(x_1) + 2f(x_2)... + f(x_n)] \tag{4}$$

3 The Finite Element Model

It is important to establish a baseline model, which can then be used to determine the relevant parameters in the spall scenario. A single Steven test from reference paper Gruau et al. (2009) is rebuild in a Finite Element Program. Used programs include LS-Prepost (version 4.8), LS-DYNA(version smp d R11.1.0), and Python (version 3.0) for the post processing phase.

3.1 Set-up of the Model

The model set-up is taken from Gruau et al. (2009). The test is a Steven test, where a steel projectile is launched towards a steel plate containing energetic material, see Figure 6. This specific test was chosen since the target plate and the projectile are circular, which is necessary for an axisymmetric (2.5 D) analysis.

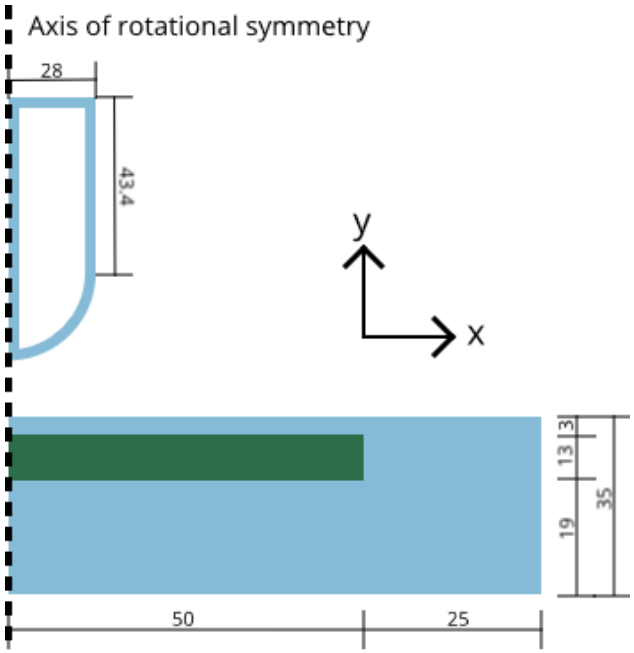

Figure 6: Geometry of the set-up including dimensions in mm. Based on the measurements and weight of the projectile in Gruau et al. (2009) and Picart et al. (2013). The dimensions of the projectile were determined using the weight given in the paper. All blue parts indicate steel, either the target or the projectile. The green part is the energetic material.

According to table 3 in the paper, the lowest reactive velocity was 77 m/s. This velocity will be used for the baseline model. The highest non-reactive velocity was 61 m/s. This means that the former should produce enough hot spots capable of a reaction, and the latter should produce significantly fewer reacted elements. Both of these projectile velocities will be investigated in this thesis.

3.2 Material Properties

Only two material models were used in this analysis: a steel bilinear model and a Drucker-Prager model for the energetic material. The projectile and target plate were assumed to be the same material, because Gruau et al. (2009) did not specify different material properties for the two steel parts.

3.2.1 The Projectile and the Target Materials

To model the steel material, MAT_003 from LS-DYNA was used. This is a bilinear material model. The properties can be found in Table 1.

Material	Density ρ	Young's Modulus (E)	Poisson's Ratio (ν)	Plastic Yield Stress (f_{ypl})
Steel	7850 kg/m^3	210 GPa	0.3	400 MPa

Table 1: Properties of the steel used in the verification set-up. Implemented in LS-DYNA using material 003: MAT_PLASTIC_KINEMATIC. This gives a bilinear model with a horizontal yielding plateau (ETAN = 0), more commonly known as ideal plasticity. Chosen to use isotropic hardening (BETA = 1).

3.2.2 The Energetic Material

The energetic material properties are based on a Drucker-Prager material model. The reference paper (Gruau et al., 2009) explains a modified material model to model the material properties of the PBX. This is too detailed for the simplified approach of this thesis. Therefore, a regular Drucker-Prager material model, as can be found as MAT_193 in LS-DYNA, is used in this thesis. This assumption does lead to some important differences, see Section 3.5.

Most of the properties could be taken directly from Gruau et al. (2009), only the cohesion value had to be derived. The cohesion can be determined using the angle of friction and the compressive strength f_c (De Borst and Sluys, 2015), see equation 5. An overview of all the values can be found in Table 2.

$$c = \frac{1 - sin(\phi)}{2 * cos(\phi)} * f_c = \frac{1 - sin(0.3491)}{2 * cos(0.3491)} * 5 * 10^6 = 1.751 * 10^6 Pa \tag{5}$$

Material	Density (ρ)	Shear Modulus (G)	Poisson's Ratio(ν)
PBX-9501	1800 kg/m^3	1.429*10^9 Pa	0.4
Angle of Friction (φ)	**Cohesion Value (c)**	**Dilation angle**	
0.3491 rad	1.751*10^6 Pa	1.745*10^{-2} rad	

Table 2: Properties of the PBX used in the verification set-up. Implemented in LS-DYNA using material 193: MAT_DRUCKER_PRAGER.

3.3 The Finite Element Model

LS-DYNA was used for the analysis and LS-PrePost was used for the pre- and post-processing of the FEM data. The geometry and dimensions as seen in Figure 6 were used in the FEM. The original test set-up was circular, meaning that an axisymmetric model is an efficient way to model the test set-up. See Figure 7 for the completed model in LS-PrePost.

Only one third of the energetic material is processed by the Python script, as indicated by the white elements in Figure 7. Only the elements close to the the middle of the test set-up are likely to react (Gruau et al., 2009). In this thesis' model that would be the area around the axis of symmetry. Therefore, the assumption is made that only a part of the energetic material was likely to react to save computation time. This assumption is evaluated later in this section, and proven valid in Section 3.4.

For an in depth look at the finite element model, the keyword file for the first analysis is included in Appendix B. The model consists solely of axisymmetric solid elements and is revolved around the y-axis as seen in Figure 7. Table 3 shows the most important choices regarding the elements used in the analysis.
As for the boundary conditions, most edges are free edges with a few exceptions:

- The bottom edge is fully clamped, it is restricted in the X, Y, Z, RX, RY and RZ directions.
- The edge along the axisymmetric Y axis is restricted in the X, Z, RX, RY and RZ directions.

Element Type	Axisymmetric solid - area weighted
Element Size	0.5 mm
Total number of elements	17952
Time Step	10 microseconds
Through Thickness Integration Points	2
Shear factor	0.833 (5/6)

Table 3: Quick overview of used elements and time step for the verification model.

A frictionless contact is defined between the projectile and the steel target. This is done using the 2D_AUTOMATIC_SINGLE_SURFACE command. All automatic/pre-set commands were used. The projectile and steel target were grouped in a set that was used to define both the slave and master surface.

There is also a contact between the energetic material and the steel target. This contact is not frictionless, but the remainder of the options is the same as discussed above. This contact definition was added because of findings in preliminary analyses. An excessive shear deformation was found along the edges of the energetic material, also leading to a high number of elements reaching the reaction criterion threshold along those edges. Since shear is such an important factor in the reaction criterion, and a lot of elements in the shear band along the top or bottom reacted, this was deemed inaccurate. To create a more accurate behaviour, a contact definition between the energetic material and the steel casing was added. Both the static and dynamic coefficient of friction were given a value of 0.5 [-]. This number was estimated and was close to found scientific data (Reaugh, 2020). This reduced the higher shear stresses along the interface between the steel and energetic material. Though it did not entirely prevent this from occuring.

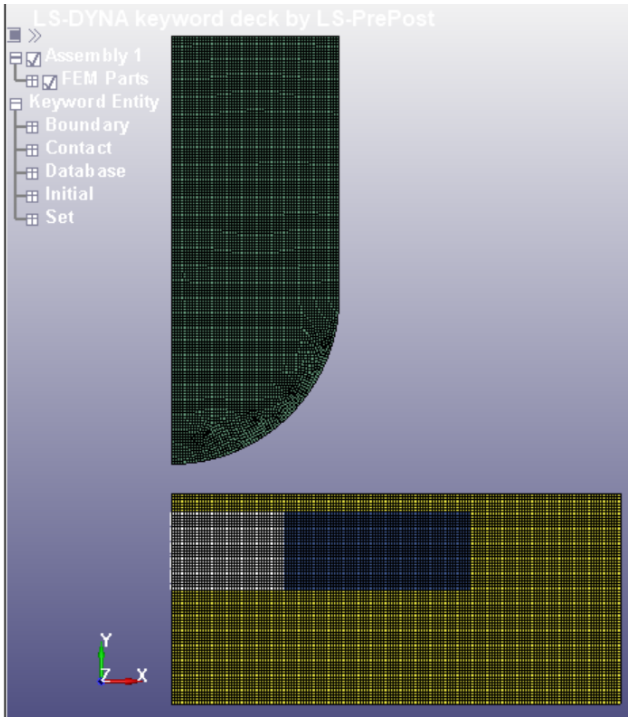

Figure 7: Finite element model as evaluated in LS-DYNA. The axis is shown in the bottom left corner. The green mesh represents the projectile, the blue and white mesh the energetic material and the yellow mesh the steel target. The white part of the energetic material shows the part that is evaluated in the post-processing phase.

3.4 Results from the Analysis

This section discusses what will be referred to throughout the thesis as the 'baseline model'. This is the model as seen in Figure 7, with a projectile velocity of 77 m/s. This will serve as the basis for the parameter study in later sections.

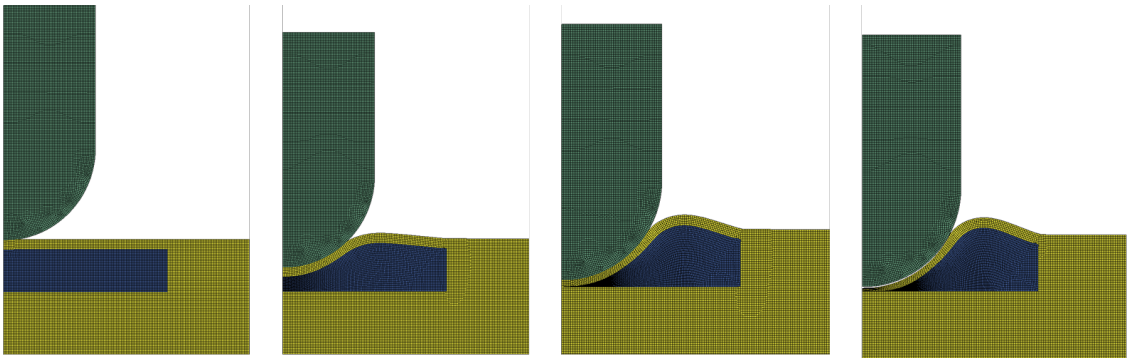

Figure 8: Deformation of the energetic material through time. Baseline model with a projectile velocity of 77 m/s. From left to right: t=30 μs (at impact), t=190 μs, t=310 μs and t=5e-4 s (end simulation).

3.4.1 Reaction Criterion in the Model

Using the Python model as described in Section 2.4, a total of 309 elements satisfy the reaction criterion with the threshold of > 1, see Table 4 for some quick results. See Figure 8 for a through time overview of the analysis.

Nr of Elements Reaching Threshold	309
Highest Pressure [Pa]	2.961e8
Highest Shear Strain Rate [-]	1.622e5
Lowest Shear Strain Rate[-]*	-5.541e4
Highest Reaction Criterion	2.477

Table 4: Results from the baseline model. The 309 elements that reacted are shown in Figure 9.

All reacted elements are close to axis of symmetry, see the white area in Figure 9. This is the case in both X and Y direction. The largest shear and pressure stresses are present in this area. This justifies only looking at the first third of the material, as was assumed earlier in this section.

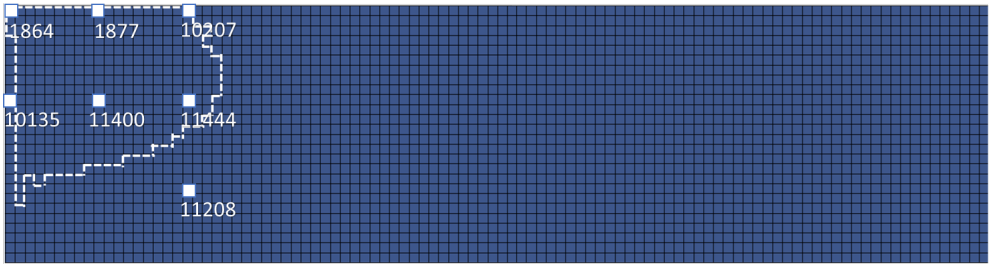

Figure 9: Position of the reacted area and different elements as shown in Figure 10. The area indicated in white encompasses all elements that reacted in the scenario where the projectile had a velocity of 77m/s.

The white elements indicated in Figure 9 are used as reference elements to show different progressions in the reaction criterion, see Figure 10). The elements are evenly spaced and are placed along the axes of symmetry and on or outside the border of the reacted material. They are also used as reference elements for future analyses in Section 4.

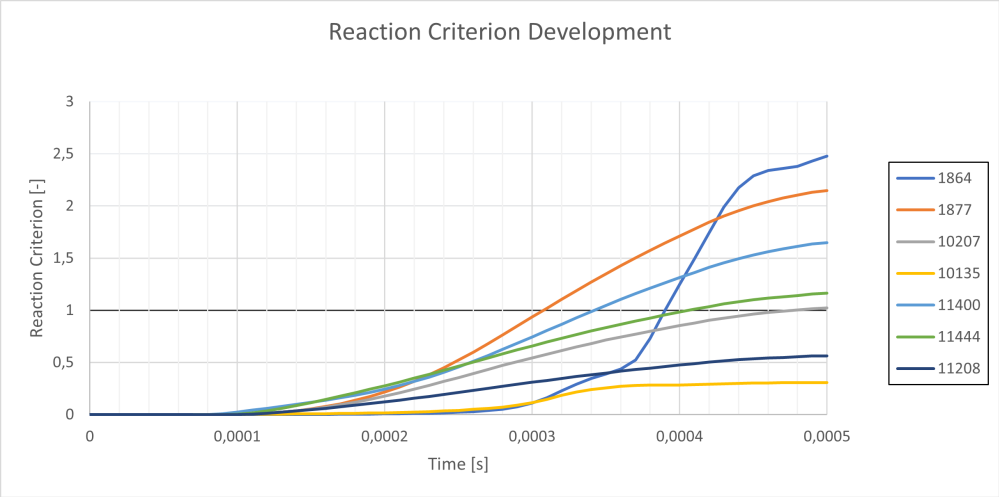

Figure 10: Plot of the development of the reaction criterion in different elements. For the placement of these elements through the energetic material, see Figure 9.

Only a small part of the energetic material is subjected to a significant xy shear, see Figure 11. Note that this is not the same as the plastic shear strain rate. However, the parts subjected to a significant xy shear are also the parts of the energetic material that develop hot spots according to the reaction criterion, see Figure 9. So it seems to be an indication for the potential of a reaction.

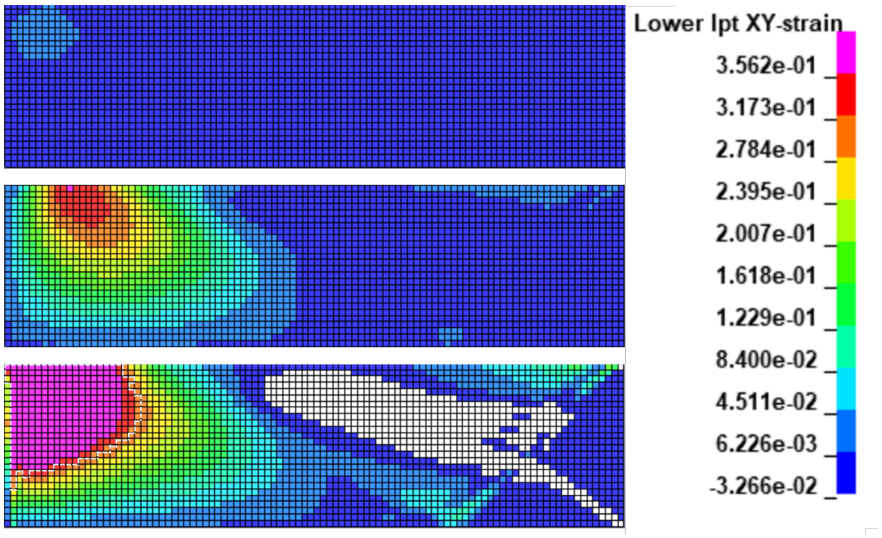

Figure 11: Shear strain development of the baseline model at different times. From top to bottom: t=70 µs, t=190 µs and t=310 µs, being the same time as the first initiations. Legends are shown on the right, y-axis is up and x-axis is to the right. The black area is the same as indicated in Figure 9. Note: White and magenta areas indicate strains/pressures that are outside the range of the legend. The legend was changed to show more detail.

Although pressure is needed in order for the reactions to develop, a high pressure alone is not enough to cause a reaction. When comparing Figures 9, 11 and 12, it is clear that areas with a high pressure, such as the entire red column on the left of Figure 12, do not necessarily lead to a reaction. This can be attributed to the plastic shear strain being very small in those specific areas.

On average, the pressure is around 10e9 times bigger than the plastic shear strain rate. So while both being larger than 0 is a prerequisite for the reaction criterion to develop, see equation 1, the pressure will contribute more to the magnitude of the reaction criterion because it is much larger than the plastic shear strain rate.

$$\frac{1}{c*}\int_0^{t_{ig}} \frac{(t_{ig}-\tau)^{-n}}{t*}\left(\frac{\langle p(\tau)\rangle}{p*}\right)^{2n/3} \dot{\bar{\gamma}}_{pl}(\tau)d\tau = 1 \tag{1}$$

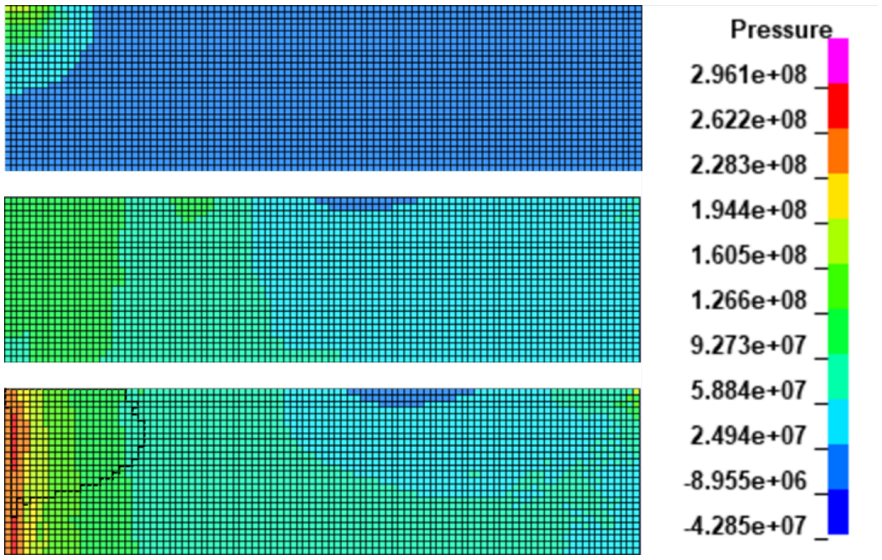

Figure 12: Pressure [Pa] development of the baseline model at different times. From top to bottom: t=70 μs, t=190 μs and t=310 μs, being the same time as the first initiations. Legends are shown on the right, y-axis is up and x-axis is to the right. The black area is the same as indicated in Figure 9. Note: White and magenta areas indicate strains/pressures that are outside the range of the legend. The legend was changed to show more detail.

Interestingly, while element 1864 (see Figure 9) does react, most elements along the axis of symmetry do not. The pressure is an contributing factor to the reaction criterion, so it seems logical that elements undergoing a large pressure will develop a significant reaction criterion. But because these elements are restrained along the y-axis they consequently cannot undergo significant shear strain. That is why most elements along the axis of symmetry do not reach the reaction criterion, see Figure 11.

3.5 Validity of the Model

The test set-up modelled in this section will lead to elements reaching the threshold of the reaction criterion. This is in line with the findings from Gruau et al. (2009). Yet when looking at Figure 13, and comparing this figure to the area in Figure 9, differences become apparent. This section will discuss some differences between the reference paper and this thesis.

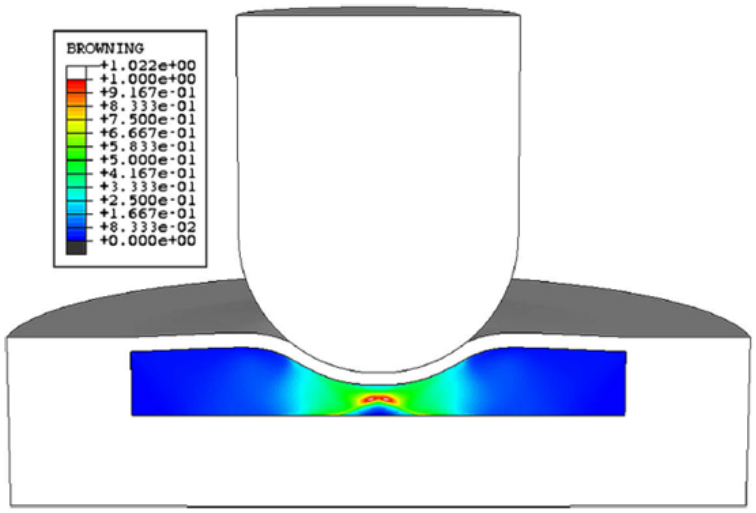

Figure 13: Figure 2 as taken from Gruau et al. (2009). 'Computational result of the target 3 test case: the left hand side of Eq. (1) is denoted by "Browning" in the legend.' 'Eq. (1)' is equation 1 in this thesis.

3.5.1 Reacted Area

The areas containing elements that reach the reaction criterion show similarities. All elements that would have reacted in the reference paper (Gruau et al., 2009) are within the area that this thesis found to react, see also Figure 14.

The area showing the highest reaction criterion does not overlap. The reaction criterion is highest in the middle of the energetic material in Gruau et al. (2009). In this research's results the highest reaction criteria can be found along the edge between the energetic material and the steel casing. This shows that the measures implementing a different contact between the steel and energetic material to prevent a larger shear force around the interface did not entirely prevent this.

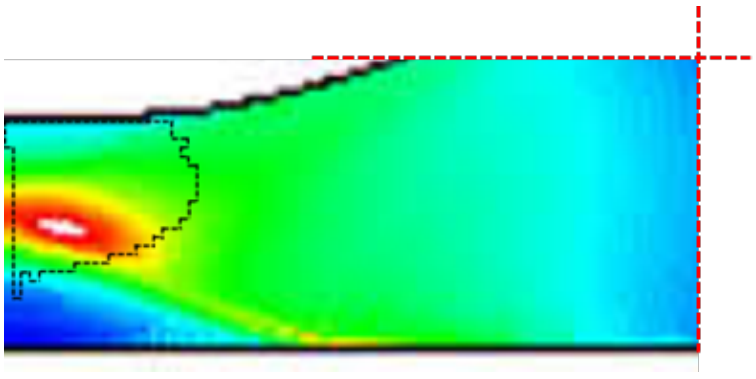

Figure 14: Rough comparison of the reacted areas in this thesis to the reacted areas in Gruau et al. (2009). The area from Figure 9 was super positioned on Figure 6. The black area shows the area of elements reaching the threshold in this thesis while the white area in the material shows the area of elements reaching the threshold in Gruau et al. (2009).

The area is much larger in this thesis than in the reference paper. The area stretches further to the axis of symmetry, to the right and up, see the figure. This has two explanations: it can be explained by the fact that the deformation in this thesis' analysis is much larger than in the reference paper, for more see Section 3.5.3. If the elements deform more, according to equation 1 the reaction criterion threshold is more likely to be reached. The other contributing factor is that the reaction criterion threshold is too low, which will be explained further in Section 3.5.2. The analysis is too sensitive, meaning that elements that should not react do reach the threshold. Lowering c* so the analysis corresponds to the tests as conducted in Gruau would make the reacted area smaller.

3.5.2 Non-Reactive Test

The tests referenced to in Gruau et al. (2009) also included the highest non-reactive velocity, namely a velocity of 61 m/s. At this projectile velocity, the specimen should not react. It is therefore expected that no elements will reach the threshold. The peak pressure and shear strain should also be lower, since the threshold combination of the pressure and plastic shear strain rate should not be reached.

Projectile velocity	**61 m/s**	**77 m/s**
Nr of Elements Reaching Threshold	160	309
Highest Pressure [Pa]	1.531e8	2.961e8
Highest Shear Strain Rate $[s-1]$	290.2	1.622e5
Lowest Shear Strain Rate $[s-1]$	-3.416e4	-5.541e4
Highest Reaction Criterion	1.511	2.477

Table 5: Results comparing the model at the lower velocity of 61 m/s to the baseline model at 77 m/s.

A significant number of elements will still reach the threshold at 61 m/s, see Table 5. The lower velocity only caused around a 50% decrease in elements that satisfy the reaction criterion. This does mean that the area of reacted elements is significantly smaller.

The reaction criterion (c*) was set at a certain value in Gruau et al. (2009), specifically based on the paper's own numerical model. The Steven-tests were used to calibrate a value for the numerical model the reference paper used. Since the paper's model is different from the model used in this thesis, see Section 3.5.3, it can be expected that the threshold for the reaction of the elements might not be the same. Table 5 shows that the c* used in the analysis could be scaled down by 1.511 to get a result where no elements reach the reaction criterion.

Some finite element analyses were run at lower velocities to check whether using the value of c* = 4.867e4 was reasonable. No elements reached the reaction criterion threshold with projectiles velocities of 30 and 50 m/s. This shows that even though this value of c* might be more sensitive than it should be, it does not lead to unreasonable results in cases that should clearly not lead to a reaction.

The value of c* = 4.867e4 is still used in this thesis. The 61 m/s is an edge case. Maybe the highest non-reactive velocity is slightly higher, but was not tested. The found reaction criteria c* are all upper and lower bound values. While they can be used to estimate the true value, it cannot be found with 100% certainty. The model does show that very low velocities do not cause any reaction, so it is accurate in clear cases. Also, the exact value of c* does not influence the underlying mechanisms of the phenomena. It is only an indication to the amount of elements that react. Therefor, the value of c* = 4.867e4 was kept the same as in the reference paper Gruau et al. (2009) for easy comparison. This causes the model to be more sensitive than it would be in reality.

3.5.3 Differences in the Material Model

As mentioned in Section 3.2, the reference paper uses a modified material model for the energetic material. A simple Drucker-Prager model was used in this thesis. This key change explains some of the more interesting differences between the two.

The material model in the reference paper is based on a concrete damaged plasticity model by Lubliner et al. (1989) and expanded upon by Lee and Fenves (1998). This model includes isotropic damage under pressure loading conditions and a yield function that is a modified version of a Drucker-Prager yield envelope

(Gruau et al., 2009). The model includes empirically found strain hardening curves and filters the fluctuating results from the finite element model. Only the Drucker-Prager yield envelope was implemented in this thesis. It was based on perfect plasticity. Implementing the full model as used in the reference paper would have been too complex for this work. So as one of the assumptions, just the Drucker-Prager model was used.

The large forces on the relatively weak energetic material (in terms of stiffness and ultimate strength) cause yielding behaviour very quickly. One of the factors contributing to the reaction criterion is the plastic shear strain rate. This means that any behaviour after elastic deformation is important, since only the plastic contribution can bring about a reaction. But this is the exact type of behaviour that could not be implemented using the simplifying assumption. Because no strain hardening could be added due to limitations in the standard Drucker-Prager model in LS-DYNA, the plastic shear strain is larger than it is in Gruau et al. (2009) and larger than it would have been in reality. Its rate will also be different. The absence of the more complicated material model therefor causes the reaction criteria to be higher.

The elastic part of the material is also modelled differently from the reference paper. This influences the pressure and the amount of force required to get a plastic deformation. Even though the contribution from shear deformation only adds to the reaction criterion when it is a plastic deformation, that does not mean that the elastic build-up is not important. Similarly, implementing a damage criterion would also have also caused a different response from the material.

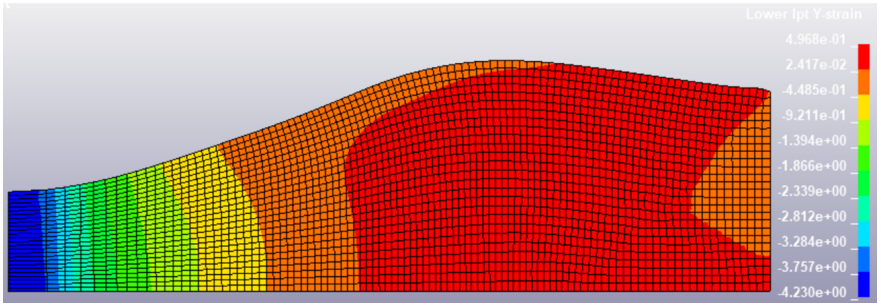

Figure 15: Deformation of the energetic material at t=310 µs in the baseline model. The shape of the figure shows the deformed state of the energetic material. Scale of the shown deformation is 0.5. The colours specifically show the strain in y direction (legend on the right), to show the excessive deformation in that direction.

The results from this finite element model also show more deformation than the paper by Gruau et al. (2009). Figures 15 and 8 show that the deformation in y-direction is quite excessive. The model deforms to the point of negative strains (see Table 4), resulting in a physical impossibility. When using engineering strain: $\epsilon = \frac{\Delta L}{L}$, ϵ can only be smaller than -1 if the element compresses more than its own length ($\Delta L < -L$). Values up to -4.23 are reached, as in the case shown in Figure 15. The elements are reduced to nothing, see Figure 8.

During the development of the reaction criterion there are large negative strains in Y-direction. This degree of deformation can be explained by the low stiffness and lack of strain hardening of the energetic material. The energetic material has a significantly lower stiffness than the steel casing and intermediate cover plate. While it does deform under the force from the projectile, it barely compresses. The steel cover plate starts compressing around t=310 µs, see the third figure in Figure 8. The energetic material in contrast, compresses virtually from the moment of impact onward.

Adding strain hardening would increase the resistance of the material to yielding behaviour. This would prevent the material to deform infinitely plastically. The material has a low Young's Modulus. This combined with the large forces on the material cause very large deformations. This strain hardening could not be included due to the chosen material properties in LS-DYNA.

The excessive deformation does not cause an energy imbalance. The losses of energy are not even 1% of the total energy. This difference is so small as to not be a cause of the excessive deformation in the analysis.

3.5.4 Time Step and Mesh Variations

To ensure the proper working of the finite element model, it is important to vary the time step and mesh size. However, in this specific model variations in the mesh size or time step cause the model to become unstable.

Mesh refinement proved to be difficult. An analysis with meshes of .25 by .25 mm was not stable. It resulted in errors pertaining to negative volumes in the elements. Refining the mesh to elements of .25 by 0.5 mm was possible. The elements were split along the y-axis, meaning that the longer side of 0.5 mm was in the direction of the y-axis. The longer side of the elements was in line with the excessive deformation direction, see Figure 16.

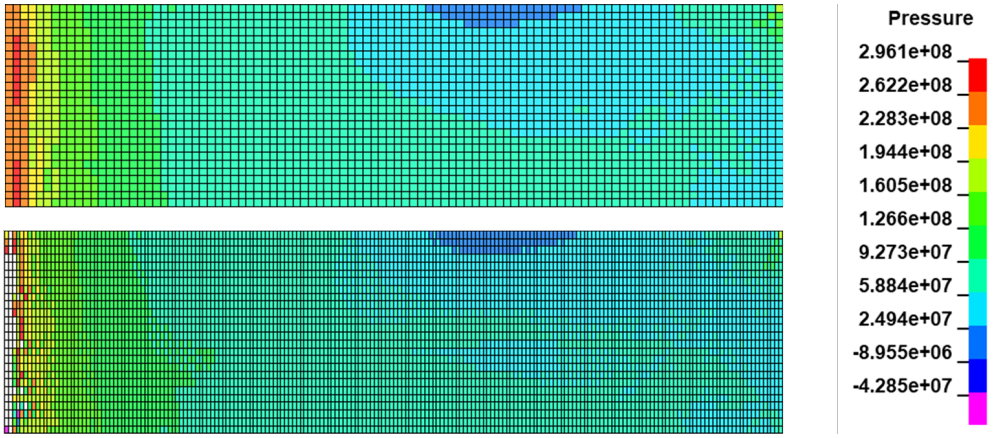

Figure 16: Pressure [Pa] at t=310 µs for the baseline (top) and refined mesh (bottom). White shows pressures higher than indicated at the legend. The refined mesh shows larger pressure around the axis of symmetry.

When looking at Figure 16, there are clear similarities between the two analyses in terms of the pressure. The green and blue areas of lower pressure on the right side of the figure show great similarities. The largest difference is around the axis of symmetry. This is also where the projectile impacts the specimen and the forces are the largest. The refined mesh shows larger forces around the axis of symmetry that are only caused by the mesh refinement.

This analysis with mesh refinement was also not stable, but still usable. It could not be completed to the end time of 500 µs as prescribed in the model. The model was terminated due to elements having a negative volume. The large deformations lead to highly distorted elements. The edges of the elements will start to overlap and cause errors in the program. Elements distorted this much can no longer be accurately mapped within a classical finite element approach. If one wants to model deformations this large, a numerical approach other than the finite element method should be used to model this behaviour.

The time step was also changed, but any change in the time step lead to an unstable analysis. Issues with the contact between the projectile and the cover plate could not be solved. Therefor the time step of 10 µs could not be compared to any other time step.

4 Parameter Study

The baseline model as discussed in Section 3 is changed to find parameters which have a dominant impact on the reaction criterion. The following parameters are taken into consideration: Projectile velocity, cover plate thickness, steel properties, compressive strength of the energetic material and the Young's modulus of the energetic material.

For a quantifiable comparison, a difference in 10% of elements that fulfil the reaction criterion is used. This is 31 elements, so if simulations have fewer than 278 elements or more than 340 elements that fulfil the reaction criterion, the change is seen as significant. If every element has a lower reaction criterion than 1.511, no reaction should take place according to Section 3.5. It is highly probable that any model that results in 160 or fewer elements that fulfil the reaction criterion do not contain a reaction. This is a 51.8 % decrease.

Throughout the parameter study, element 11400 will serve as a reference elements. This particular element lies somewhere in the middle of the reacted area of the baseline area. Element 11400 also showed clear differences between analyses to easily identify the result of the parameter change. See Figure 9 for the placement in the finite element mesh.

4.1 Projectile Velocity

On top of the variation as done in Section 3.3, a few extra velocities were taken into account for this analysis, see Table 6. The velocity can be linked to the amount of energy introduced to the test-setup since velocity is a part of kinetic energy.

Velocity [m/s]	**Nr of Elements Reaching Threshold**	**Highest Reaction Criterion**
50	0	0.991
52	8	1.054
53	45	1.098
55	76	1.199
61	160	1.511
65	201	1.720
70	262	2.048
75	294	2.380
77	*309*	*2.477*
80	319	2.898

Table 6: Shows the velocity at which the test was run and the consequently reacted elements. The baseline model with a velocity of 77 m/s is indicated in italics. Simulation for 80 m/s not finished, only last step is missing.

In contrast to the reference paper (Gruau et al., 2009), this thesis' FEM shows that a velocity of 50 m/s is the highest projectile velocity which does not cause a reaction. A higher velocity results in more reacted elements, see Table 6, and that elements react faster, see Figure 17.

Figure 17 also shows that a higher velocity results in a higher reaction criterion. If there is a margin of error in calibrating c*, the energetic material can be said to react with more certainty. The elements also reach the threshold of 1 earlier.

Figure 18 shows the development of the xy-shear in different stages of the analyses with changed velocities. The shear strain shows areas in line with the findings of table 6: The large area of shear strain from 77 m/s is roughly halved when looking at 61 m/s, and has almost disappeared in the analysis at 50 m/s.

When looking at the pressure development in Figure 19, the same conclusion as in Figure 12 can be reached: higher projectile velocities lead to higher forces in the material. The pressure is higher around the axis of symmetry. This correlates to the areas that reach the threshold of the reaction criterion. Yet the pressure is not as concentrated around the area of elements reaching the threshold of the reaction criterion as the xy-shear is.

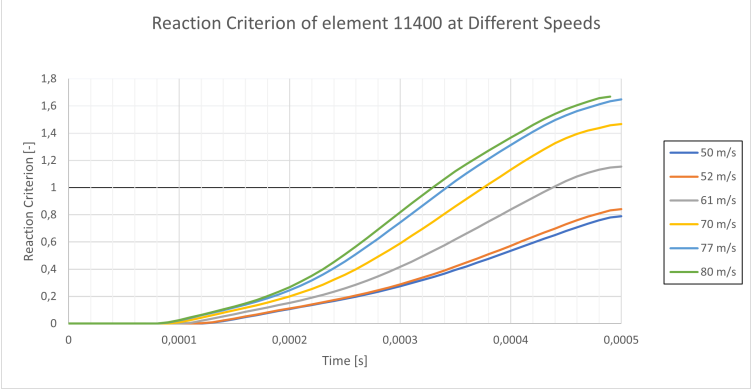

Figure 17: Plot of the development of the reaction criterion in element 11400 for different projectile velocities. 77 m/s is the baseline model. Note: the distance between the projectile and the cover plate was not changed, meaning that the higher velocity studies will have an earlier moment of impact.

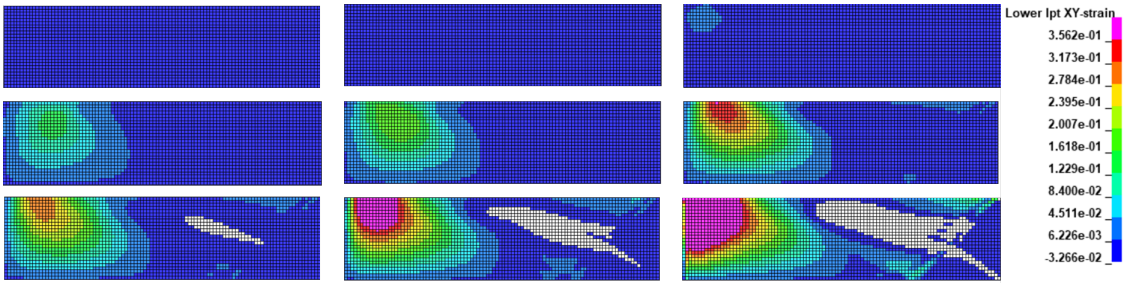

Figure 18: XY-Shear strain [-] development in the model, from left to right, at 50, 61 and 77 m/s. The different times, t=70 µs, t=190 µs and t=310 µs, are shown from top to bottom. Legends are shown on the right, y-axis is up and x-axis is to the right. Note: White and magenta areas indicate strains/pressures that are outside the range of the legend. This to make the pictures more insightful.

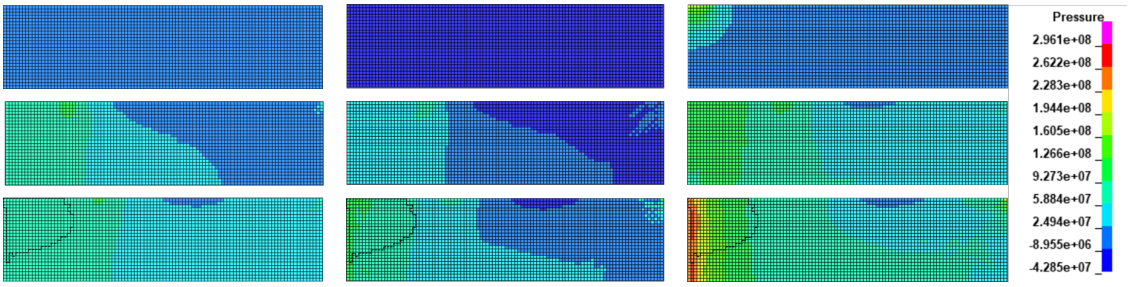

Figure 19: Pressure [Pa] development in the model, from left to right, at 50, 61 and 77 m/s. The different times, t=70 µs, t=190 µs and t=310 µs, are shown from top to bottom. Legends are shown on the right, y-axis is up and x-axis is to the right. Note: White and magenta areas indicate strains/pressures that are outside the range of the legend. This to make the pictures more insightful.

4.2 Cover Plate Thickness

Another test set-up variable that can be changed is the thickness of the cover plate. The thickness of the steel layer covering the energetic material, was changed in a couple of increments. With a spread of +0.5 mm to +10 mm, Table 7 shows the number of elements that satisfy the reaction criterion.

As can be seen in Table 7, changing the thickness of the plate has a significant impact on the number of elements that satisfy the reaction criterion. The significant change of 10% in the number of reacted elements is already reached with an increase of 0.5 mm. The number of these elements seems to decrease with a thicker cover plate, but at a thickness of 13 mm there are some elements that react. This strange anomaly

Thickness [mm]	Nr of Elements Reaching Threshold	Highest Reaction Criterion
3	*309*	*2.477*
3.5	276	2.086
6	67	1.193
6.5	24	1.073
8	0	0.8172
13	98	1.284

Table 7: Shows the reacted elements when the thickness of the cover plate is changed. The baseline model with a thickness of 3 mm is indicated in italics.

can be seen in Figure 20, where the 8 mm cover shows the lowest reaction criterion, while the 13 mm cover almost reaches the threshold again.

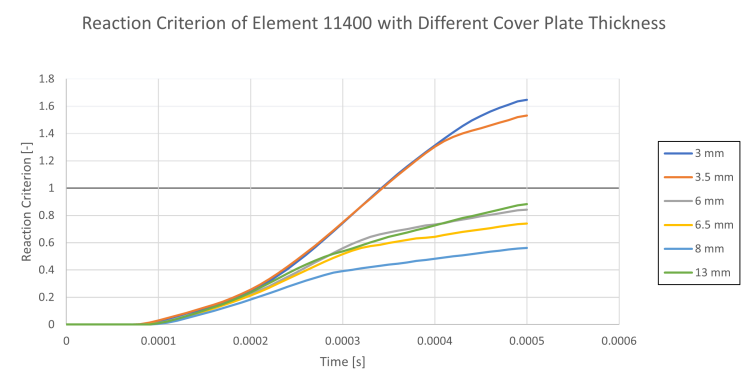

Figure 20: Plot of the development of the reaction criterion in element 11400 for different cover thicknesses. 3 mm is the baseline.

The anomaly at 13 mm can be explained by the extra stiffness of the cover plate. When looking at Figure 21, the deformation in analysis at 13 mm shows a different deformation shape of the energetic material. Since the cover plate is very thick, the material cannot expand upwards on the right side. This bulging behaviour is formed next to the projectile is smaller whenever the thickness is increased. See also Figure 8 and compare to Figure 21.

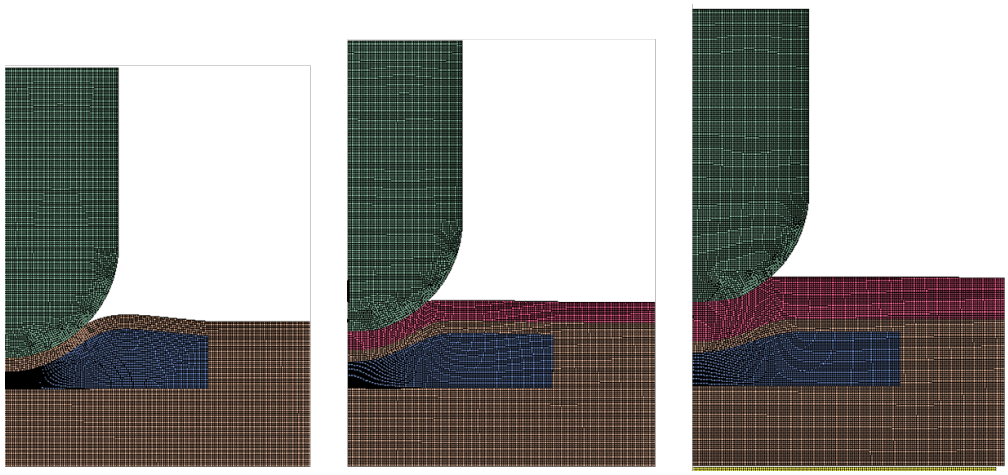

Figure 21: Analysis at time = 190 µs. Cover thicknesses from left to right are 3.5, 8 and 13 mm.

The stiffer cover plate hinders the bulging behaviour that occurs at smaller thicknesses. The material

used to deform upwards, but due to the thicker cover plate is not able to do so. This explains the heightened pressure as seen in Figure 23, these are higher confining pressures. The trend of higher plateau like pressures between 100 µs and 300 µs shows that a thicker cover plate leads to higher pressures. The higher (in absolute terms) plastic shear strain rate can be seen in Figure 22. The progression shown in Figure 21 shows that the cover does not deform as much.

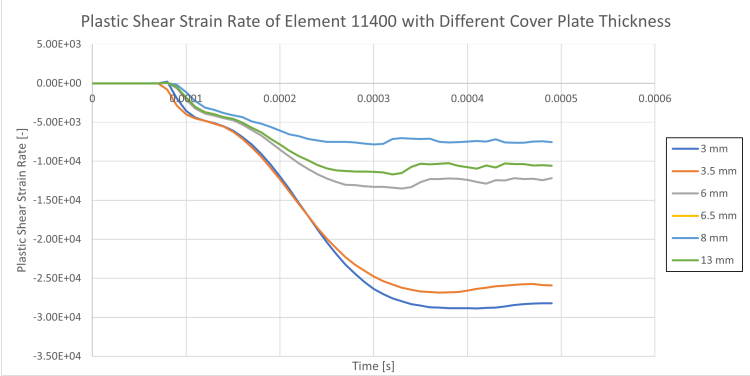

Figure 22: Plastic Shear (xy-shear) strain rate [-] plot of element 11400 with varied cover thickness. In this specific graph, the lines of 6.5 and 13 mm overlap in such a way that 6.5 mm in not visible.

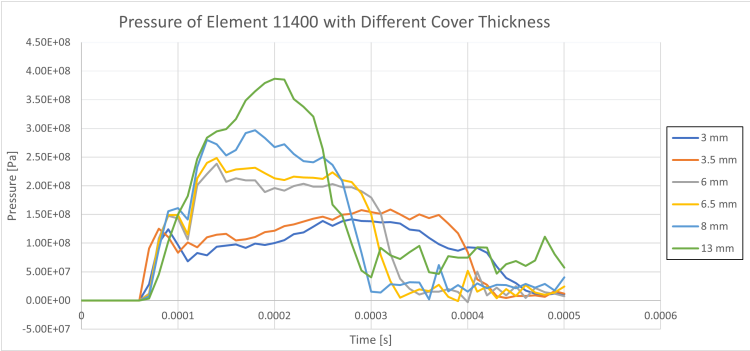

Figure 23: Pressure [Pa] plot of element 11400 with varied cover thickness.

4.3 Properties of the Steel Material

The material properties of the steel parts were also changed. The chosen steel types were based on expert opinion. These specific changes were chosen in such a way that the steel properties in the test set-up can be compared to the steel properties commonly used in ammunition articles. Though, this means that not one, but multiple characteristics, such as the yield strength and the Young's Modulus, of the material were changed at once, see Table 8. So the parameter change contains two changed variables, making it difficult to determine if the Young's modulus or the yield stress is more impactful.

Name	**E [GPa]**	**fy [MPa]**	**Nr of Elements**	**Highest Reaction Criterion**
Baseline	210	400	309	*2.477*
Steel type 1	200	220	245	2.123
Steel type 2	200	330	322	3.169

Table 8: Shows differences between different analysis and the reacted elements for each analysis with changed material properties.

A note on this parameter change can be made regarding the fact that both the projectile and the cover plate are made of the same material. In practice, this will not be the case.

Table 8 shows that the weakest steel type causes the fewest number of elements to react. This might be due to the fact that the steel itself can deform more, see Figure 24. The yield strength of the cover plate is reached at an earlier time step. This results in the steel cover plate to take up more energy from the impact. This means that less energy from the impact will eventually reach the energetic material. However, most elements reach the threshold criterion well before the end of the analysis, but the flattening of the projectile only happens at the very end. So the fact that the steel projectile can take up more of the impact loading does not change the reaction criterion that much.

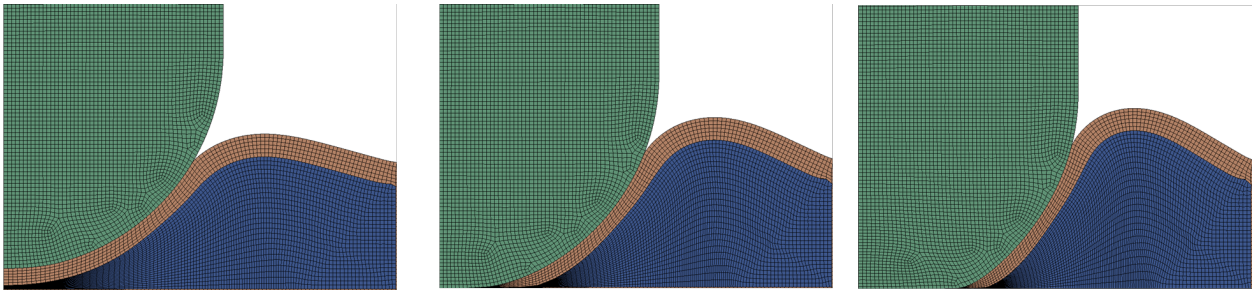

Figure 24: Deformation at t=2.7e-4 s, t=3.4e-4 s and t=4.4e-4 s, the last being the end of the analysis. The projectile flattens in the final figure, it does not do so in the other steel type analyses.

A different explanation of the lower number of elements reaching the reaction criterion threshold in steel type 1, can be seen in Figure 25. The analysis for steel type 1 was cut short due to an instability in the analysis creating negative volume in one of the elements, which caused an unstable analysis. This means that elements that would have reacted later on in the analysis, were not taken into account in the number as shown in Table 8.

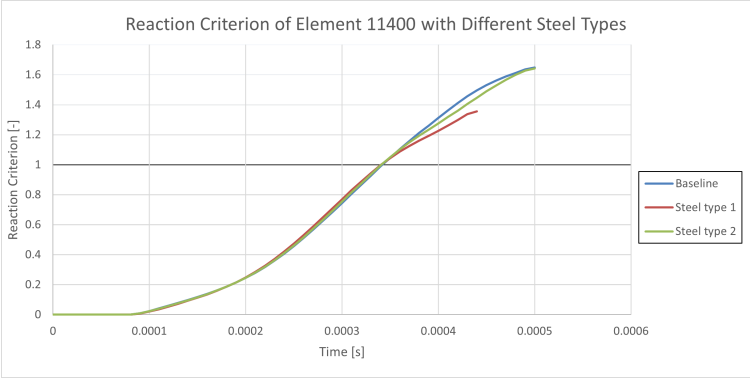

Figure 25: Plot of the development of the reaction criterion in elements 11400, comparing the baseline model with commonly used ammunition materials.

4.4 Compressive Strength of the Energetic Material

The compressive strength (f_c) can be varied in the model. This might alleviate some of the excessive deformation in the energetic material. f_c in equation 6 (De Borst and Sluys, 2015) is varied by changing the cohesion factor in the material model. Keeping ϕ the same, the only change should be to f_c.

$$c = \frac{1 - sin(\phi)}{2 * cos(\phi)} * f_c \tag{6}$$

f_c [MPa]	Nr of Elements Reaching Threshold	Highest Reaction Criterion
5	*309*	*2.477*
7.5	304	2.461
10	302	2.344
15	291	2.189
20	283	2.123
25	262	2.005

Table 9: Shows the reacted elements when the compressive strength (f_c) is changed. The baseline model with an $f_c = 5MPa$ is indicated in italics.

When looking at Table 9, it shows that a higher compressive strength leads to fewer reacted elements. This effect is small when comparing the change in results of different parameters with a relatively smaller change. Doubling, tripling or even quadrupling the compressive strength does very little to change the behaviour of the energetic material. This is also clear from Figure 26, where all reaction criterion reach the threshold value at around the same time.

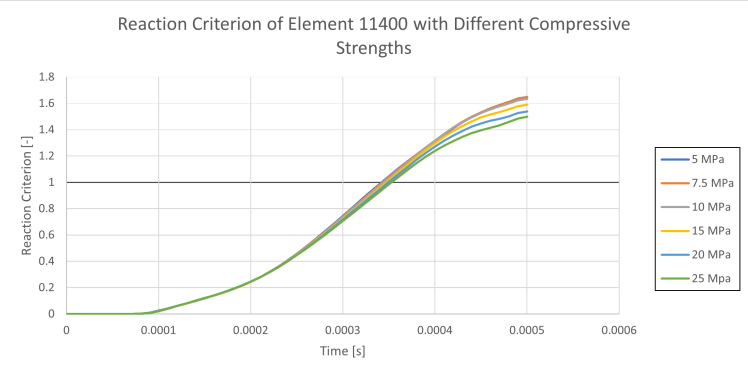

Figure 26: Plot of the development of the reaction criterion in element 11400 for different compressive strengths.

4.5 Young's Modulus of the Energetic Material

A higher Young's modulus means that there will be less elastic deformation under the same amount of stress, see equations 2 and 3. However, the difference is very small, see Figure 27 an Table 10

E [GPa]	G [GPa]	Nr of Elements Reaching Threshold	Highest Reaction Criterion
4	1.429	*309*	*2.477*
8	2.857	303	2.392
16	5.714	306	2.329
24	8.571	300	2.263

Table 10: Shows the reacted elements when the compressive strength Young's modulus is changed. The corresponding Shear modulus has also been given. The baseline model with $E = 4GPa$ is indicated in italics.

This small change in the number of elements that reach the threshold can be explained by the small contribution of the elastic shear strain to the total shear strain. When looking at the baseline model, the contribution of the elastic shear strain is 7% of the total shear strain. Compared to the excessive plastic deformations in the material, changing the elastic material properties does not influence the overall behaviour of the material that much.

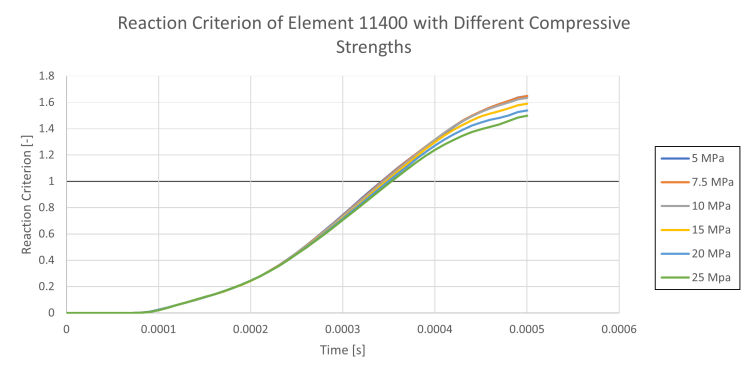

Figure 27: Plot of the development of the reaction criterion in element 11400 for different Young's Modulus.

4.6 Significant Parameters

An overview of the changes that reached the 10% significance threshold is summarised in Table 11. The baseline model showed 309 reacted elements with a highest reaction criterion of 2.477. It is interesting to note that the highest reaction criterion and the number of reacted elements do not entirely correlate. The largest change in the number of elements that reacted, namely the steel type, also had the highest reaction criterion.

Variable	Change in Nr of Elements Reaching the Threshold	Relative Parameter Change	Highest Reaction Criterion
Velocity	-47	-9.09%	2,048
Cover Plate Thickness	-33	+16.7%	2,086
Steel Type	-64	- *	2,123
Compressive Strength	-47	+500%	2,005

*Table 11: Shows the parameters that had a significant change (more than 10%) in number of reacted elements. This table only includes the smallest change to the model needed to reach an effect in the number of reacted elements of 10%. * The Steel Type saw a change in Young's Modulus (+4.8%) and the yield strength (-45%) of the material and cannot be summarised in a single percentage.*

Changing the material properties of the energetic material does not have a significant impact. Changing the Young's modulus does not show a significance change at all, and increasing the compressive strength of the material by 500% has the same, or smaller influence, than other parameters. This does not even consider the fact that the material properties cannot be changed very easily. The munition article might also no longer function properly if material properties are changed too much.

Changing the velocity of the projectile is highly effective. However, this is not a very practical solution to making ammunition articles more resistant to initiation due to impact. The projectile velocity is not determined by the ammunition article, but its surroundings. This means that this is more relevant information for e.g. designers of storage magazines than for designers of ammunition articles.

Changing the cover plate thickness is also highly effective. Increasing the thickness with 0.5 mm is already enough to decrease the number of elements that will reach the reaction criterion by more than 10%.

One of the two different steel types also caused a decrease in reacted elements by more than 10%. The new steeltype was a combination of changes in the Young's Modulus and the yield strength in the steel material. Since two different variables, the Young's Modulus and the yield strength, were changed, it cannot be said which of the two variables contributed the most.

5 Discussion

This discussion is split into three parts. The first part of the discussion covers general points of discussion. The second part of the discussion covers the assumptions underlying the model. Finally, the suitability and stability of the model is discussed.

5.1 General Discussion Points

The model was based on a large number of discretisations and numerical approximations. First: a finite element model is always a discretisation. Second: the integral was numerically computed. Third: manual inputs were required at the moment of impact during the post-processing of the data. At time of impact the contribution to the reaction criterion was so high as to cause processing problems. The choice was made to set the first contribution to the reaction criterion at zero at time of impact, see Appendix A and Section 2.4.1. Fourth, the used theoretical model (Browning, 2002; Browning and Scammon, 1995) implicitly uses averages and numerical approximations. So each layer of the model deals with small inaccuracies or rounding off errors. These factors might make a difference for some individual elements, but not for the overall picture of the analysis.

Finding good visual representations for clear comparisons was difficult. There was no easy way to visualise the reacted elements in LS-Prepost because an external program was used to find the reaction criterion. This meant that, in order to visualise the reacted area, each reacted element had to be manually entered into LS-Prepost. A similar restriction applied to the plastic shear strain rate. Only the XY-shear could be visualised. This is a close substitute, but not as insightful as immediately seeing the plastic shear strain rate. It would have been possible to develop a separate Python tool to visualise these outcomes, but this was too labour intensive for this specific research. More knowledge on the exact locations and areas of the reacted elements and relevant forces could have proven insightful for the phenomenon at large.

The problem discussed in this thesis is extra complex because it is a combination of two very different fields of study. Some assumptions in one area are difficult to translate to the other area. The combination of chemistry and mechanics, makes it difficult to check the validity of some assumptions if the researcher is more familiar with only one of the fields.

5.2 Assumptions

During modelling, it was assumed that the reaction would take place within 500 µs. This was the preset time to terminate in the LS-DYNA model and was based on the reference paper (Gruau et al., 2009). For some of the analyses, the time to impact was not taken into account, so the time was even shorter than that. However, the complete interaction always took place within that time frame. At the end of each simulation, the projectile was no longer touching the cover plate. This means the assumption that no additional elements will react after 500 µs was reasonable, since no external forces are working on the energetic material after that time.

This model also assumed that reacted elements behave the same as non-reacted elements. The chemical properties are only taken into account during the post-processing stage. It was assumed that each reacted element would generate a self-sustaining reaction that would spread throughout the material. This means that once a single element has reached the threshold, the entire material will react. So the interaction with forces generated from the reaction will not cause any different result, since the entire energetic material will react anyway.

The material model was assumed to be a Drucker-Prager model. This was only a part of the material model from the reference paper. This assumption meant that strain hardening behaviour could not be added to the model, since it was unavailable within the Drucker-Prager material in LS-DYNA. This assumption made it more difficult to capture the actual behaviour of energetic materials, as discussed in Section 3.5.3. Since internal forces cause the reaction, this assumption has a large influence on the outcome of the analysis. In this case, it was also responsible for the excessive deformation and thus partly responsible for the instability of the analysis. The accuracy lost is not only with the material behaviour after yielding, but also during the elastic portion of the response. Though it made the method much more simple to execute, it prohibited capturing a more accurate response from the material.

Within this thesis the assumption was made in an early stage to use the same c* as the reference paper (Gruau et al., 2009), see also Section 3.5.2. However, due to differences in the material models in the finite element analysis, c* should have been calibrated to this specific computational model. Dividing c* by 1.51, as found in Section 3.5, would have influenced the number of elements that reached the reaction criterion threshold. If the number of elements that reach the threshold is an indication about the nature of the reaction, that would make it useful information. But it is unknown if that is the case. What can be said with more precision however, is that no reaction will occur when the threshold is not reached. And in that case, c* is merely a scaling factor. The highest reaction criterion values show which simulations would not have caused a reaction with a different c*.

5.3 Suitability and Stability of the Model

The deformation of the energetic material in the finite element model is excessive. Even during analyses with an increased stiffness of the energetic material, the material still deforms to a large degree, as seen in Figure 15. That is partly due to modelling PBX-9501: this type of energetic material has a very low stiffness and the forces exerted by the projectile are very large.

Complex mechanical behavioural models, like strain hardening or damage criterion, are also not included. Section 3.5 shows that there are significant differences between the material models of this thesis and the reference paper (Gruau et al., 2009). This contributed to the large deformations in the material.

The large deformation in the elements caused highly distorted elements. Eventually leading to instability in analyses that changed the time step, mesh or another parameter. There is only a very small time step and mesh size range where the analysis is stable. The time step size or mesh size should not have a significant impact on the analysis or cause instabilities.

The large deformations are inevitable due to the high forces on the material. Some material changes might mitigate the tendency towards instability, but it is also likely that the finite element method is not suitable to model the behaviour. If the large deformations are a respresentation of reality, the finite element method is not able to capture the behaviour without becoming unstable. If the material really behaves like this, it is important to look at other ways of computationally modelling the set-up.

6 Conclusions and Future Research

The section is split into two parts: a conclusion answering the main and sub-questions of this thesis and recommendations for future research.

6.1 Conclusion

The main question of this research is: *Which parameters are dominant in preventing a reaction in a munition article subjected to a crushing type loading?* Section 4.6 shows that the velocity needs the smallest adjustment to result in a significant change. Increasing the thickness of the cover plate is also highly effective in reducing the number of elements satisfying the reaction criterion. Changing material properties, like the compressive strength of the energetic material or the properties of the steel is not as effective. Proportionally, a larger change is necessary to get the same decrease.

The model as described and executed in this thesis gives a first indication of influential parameters. The post-processing Python script works as desired and can be combined with future models. From the vantage point of developing a simplified engineering approach, manually developing a material model was not within the scope. Though this did lead to instability. Due to the instability of this model, it is not recommended to continue research using this specific simplified material model. This research shows that with simple tools a small insight into the development of the reaction criterion can be found. It also shows that simple tools do not lead to stable solutions and lead to uncertainties in the results that are too large to use for continued research.

6.1.1 Which simplifications can be made to create a model?

The simplified material model leads to some computational issues. These include instability of the model, excessive deformation and a more sensitive result. Incremental changes in the time step or mesh size can lead to highly distorted elements, leading to instability. This is not acceptable in a numerical model. Both because it limits the changes one can make during a parameter study, but also because it is more difficult to check the accuracy and convergence of the model. This simplification of the material behaviour was a wrong assumption. The material model could have been more complex to better predict a reaction, as was discussed in Section 5.2.

Other simplifications, like modelling the energetic material as homogeneous, are a part of the chemical model to predict a reaction. Those assumptions cannot be changed for the reaction criterion to still work. So these assumptions/simplifications were unavoidable when during modelling.

It was a suitable choice to exclude any mechanical response from elements after they reacted. Firstly, it would have added to the complexity of the problem since much more knowledge of chemical processes was needed. It would also have required multiple analyses, since the reaction criterion was processed outside of LS-DYNA. Secondly, since the chemical model implies that the elements reaching the reaction criterion threshold spread their reaction. This means that once an element reacts, the spreading of the chemical reaction throughout the material is of greater importance than any residual internal mechanical behaviour.

6.1.2 Which loading parameters on the munition article are the most critical in preventing or allowing a reaction?

The most critical external parameter is the velocity of the projectile. This is a logical conclusion, since it directly relates to the amount of pressure and strain in the energetic model. These two internal parameters form the conditions under which the reaction criterion is able to develop. If either is 0, the reaction criterion will not develop at all. Of the two, the pressure contributes the most to the development of the reaction criterion. However, other factors such as the weight or size of the projectile were not a part of the parameter study. So it is not possible to say this was the most important external parameter, since it was the only external parameter that was researched.

6.1.3 Which munition article properties are the most critical?

Increasing the cover plate thickness, or in practice the casing thickness, is a very effective way to make the set-up less sensitive. This research's specific test set-up does suggest that it should only be done sparingly to prevent an excessive build up of confining pressure. Whether this will also happen in practice in munition articles cannot be said for certain, but might very well be a factor to take into account. Material changes, like the compressive strength of the energetic material, can be applied, but will need larger relative changes.

Generally, the changes that can be made to the munition articles should not impact the functioning of the munition article. It will be difficult to design a new munition article with only one specific design element changed. There are other important factors apart from the sensitivity of the munition article to spall that complicate changing a very specific parameter. Maybe the PBX composition can be changed to get a higher compressive strength, but this could mean a different binder to granule mixture or a different kind of binder. These type of changes can change the force of the blast or the fragmentation of the munition article, effectively changing the very purpose for which munition articles are designed.

6.2 Future research

In future research, the energetic material model should be more accurate and detailed. Specifically, hardening behaviour should be included in the model. On top of that, a Drucker-Prager model is likely too simple to capture the behaviour of the material, so a more complex material model for the general behaviour is also needed. This includes e.g. strain hardening, more accurate loading curves or simulated damage. This can partially mitigate the unstable response.

More detailed material models need more research into the mechanical properties of HMX-like explosives, since the data is scarce. Future research can focus on testing and subsequently modelling PBX's with more detail, but could also include other types of explosive material. Gaining more insight into PBX's specifically can include modelling it as a heterogeneous material consisting of granules and binder. This type of research is purely to gain more insight into the mechanical behaviour of the material. Being able to translate those properties into a finite element model will also need future research.

Estimating c* is very difficult when analyses do not have a one to one representation in field tests. Future research should investigate whether keeping the material model the same results in a c* that is constant for different test set-ups. This is a prerequisite for models that are used to predict a reaction instead of validate a field test. If this model is used to find the sensitivity of munition articles without testing on those munition articles, the value of c* should be consistent over different models.

A very practical goal for future research is being able to add more detail to the classification of sensitivity groups (SG) in regulations. Future research can be used to work towards a full 3D analysis of a munition article. This way, real-life munition articles can be tested in realistic scenarios. Firstly, the model should be more accurate. This includes energetic material parameters, but also verification if c* can be kept the same if the same material model is applied, but used in a different context. This might need considerable research. Secondly, more should be known about the conditions of spall loading. This was outside the scope of this research, but there is not a lot of data on the nature of spall and for realistic risk analyses the loading on the munition articles should be well defined. Thirdly, is that future research should focus on finding stable solutions in their analyses. A stable solution that is not significantly influenced by mesh refinement or time step reduction is necessary to conduct extensive comparisons and validate the model.

References

Antoun, T., Curran, D., Razorenov, S., Seaman, L., Kanel, G. I. and Utkin, A. V. (2003), Spall fracture, Springer, New York.

Barua, A. and Zhou, M. (2011), 'A lagrangian framework for analyzing microstructural level response of polymer-bonded explosives', Modelling and Simulation in Materials Science and Engineering **19**(5), 055001.
URL: *https://doi.org/10.1088/0965-0393/19/5/055001*

Bowden, F. P. and Yoffe, A. D. (1985), Initiation and growth of explosion in liquids and solids, Cambridge science classics, Cambridge University Press, Cambridge ;.
URL: *http://catdir.loc.gov/catdir/description/cam031/85047912.html*

Browning, R. V. (2002), Microstructural model of mechanical initiation of energetic materials, in 'AIP Conference Proceedings', Vol. 370, American Institute of Physics, pp. 405–408.

Browning, R. V. and Scammon, R. J. (1995), Microstructural model of ignition for time varying loading conditions, in 'AIP Conference Proceedings', Vol. 620, American Institute of Physics, pp. 987–990.

Chidester, S. K., Green, L. G. and Lee, C. G. (1993), 'A frictional work predictive method for the initiation of solid high explosives from low-pressure impacts'.

Cooper, P. W. and Kurowski, S. R. (1996), Introduction to the technology of explosives, VCH, Cambridge.

De Borst, R. and Sluys, L. (2015), Computational Methods in Non-linear Solid Mechanics, Delft University of Technology.

Ellis, K., Leppard, C. and Radesk, H. (2005), 'Mechanical properties and damage evaluation of a uk pbx', Journal of materials science **40**(23), 6241–6248.

Field, J. E. (1992), 'Hot spot ignition mechanisms for explosives', Accounts of chemical Research **25**(11), 489–496.

Gruau, C., Picart, D., Belmas, R., Bouton, E., Delmaire-Sizes, F., Sabatier, J. and Trumel, H. (2009), 'Ignition of a confined high explosive under low velocity impact', International Journal of Impact Engineering **36**(4), 537–550.
URL: *https://www.sciencedirect.com/science/article/pii/S0734743X08002182*

Handley, C. A. (2012), 'Critical hotspots and flame propagation in hmx-based explosives', AIP Conference Proceedings **1426**(1), 283–286.
URL: *https://aip.scitation.org/doi/abs/10.1063/1.3686274*

Lee, J. and Fenves, G. L. (1998), 'Plastic-damage model for cyclic loading of concrete structures', Journal of engineering mechanics **124**(8), 892–900.

Liu, R. and Chen, P. (2018), 'Modeling ignition prediction of hmx-based polymer bonded explosives under low velocity impact', Mechanics of Materials **124**, 106–117.

Lou, J., Zhou, T., Zhang, Y. and Zhang, X. (2017), Numerical simulation study on thermal response of pbx 9501 to low velocity impact, in 'AIP Conference Proceedings', Vol. 1793, AIP Publishing LLC, p. 030021.

Lubliner, J., Oliver, J., Oller, S. and Oñate, E. (1989), 'A plastic-damage model for concrete', International Journal of solids and structures **25**(3), 299–326.

Manner, V. W., Yeager, J. D., Patterson, B. M., Walters, D. J., Stull, J. A., Cordes, N. L., Luscher, D. J., Henderson, K. C., Schmalzer, A. M. and Tappan, B. C. (2017), 'In situ imaging during compression of plastic bonded explosives for damage modeling', Materials (Basel) **10**(6).

North Atlantic Treaty Organization (2015), 'NATO Standard AASTP-1 NATO Guidelines for the Storage of Military Ammunition and Explosives'.

Picart, D., Ermisse, J., Biessy, M., Bouton, E. and Trumel, H. (2013), 'Modeling and simulation of plastic-bonded explosive mechanical initiation', International Journal of Energetic Materials and Chemical Propulsion **12**(6), 487–509.

Ravindran, S., Tessema, A. and Kidane, A. (2016), 'Local deformation and failure mechanisms of polymer bonded energetic materials subjected to high strain rate loading', Journal of Dynamic Behavior of Materials **2**(1), 146–156.
URL: *https://doi.org/10.1007/s40870-016-0051-9*

Reaugh, J. E. (2020), Applying the hermes model to non-shock ignition and post-ignition violence, in 'AIP Conference Proceedings', Vol. 2272, AIP Publishing LLC, p. 050024.

Scholtes, G. and Verbeek, R. (2010), Simulation and low velocity impact testing on confined explosives, Report, TNO.

Stewart, J. (2012), Calculus : early transcendentals, Brooks/Cole, Cengage Learning.

Wees, R. V., Tscholakov, J. and Landmann, F. (2007), Defence trial 845/03 - acceptor magazine test, Report, TNO.

A Python Script

Script made using Jupyter Notebook, used version: Python 3.

1 Python script for evaluating a reaction criterion

[ ]:
```
import numpy as np
import matplotlib.pyplot as plt
import csv
import pandas as pd
```

Some notes on the script:

The input files have to be very specific. If the input file has a different sequence, wrong columns or rows might be dropped. So check the dataframes after each section

Names should be automatically generated: stress for hydrostatic stress, strain for the strain and strain rate for the strain rate

Generally speaking:
-a is used to define the length of a for loop, calculated using the amount of columns in the dataframe
-d is used to drop columns from the dataframe
-The different dataframes generated in this notebook are: trial, de, dfs, de, del, dfpl, dataframestress, dataframstrain, Dataframe, ReactCrit and IntValue.
-For a quick summary of the reacted elements, the final cells give and count them
-This file is meant for Axi-symmetric simulations since only the xy shear is taken into account

2 Choosing Input File Names

[ ]:
```
newname = 'Reaction criterion output.xlsx'

filenamepressure = 'Pressure'
filenamestrain = 'elShellUpEps'
filenamestress = 'elShellStressIp0001'
```

3 Generate Element Number List

[ ]:
```
trial = pd.read_csv('elShellUpEps_desc', names = ['column'], header = 4,␣
 ↪usecols=[0]) #import file, skip lines not containing element numbers

trial[['entry', 'Element number', ' type', 'unit']] = trial.column.str.rsplit('␣
 ↪', 3, expand=True)

a = trial['Element number'].to_numpy() #create array from the only column that␣
 ↪is needed

x = 3 #data per element, 3 now since it is xx, yy, and xy

c = int(len(a)/x)
```

```
element_list = []
for i in range(c):
    element_list.append(a[i*x])

elementnr = len(element_list)

# print(len(element_list))
```

4 Strain File Manipulation

[ ]:
```
strain = np.genfromtxt(filenamestrain)
de = pd.DataFrame(strain)
```

[ ]:
```
a = int((len(de.columns))/3)

strainname = ['Time']
stressname = ['Time']
elasticstrainname =[]
d = []

for i in range(a):
    strainname.append('strain {}'.format(i+1))
    stressname.append('shear stress {}'.format(i+1))
    elasticstrainname.append('Elastic shear strain {}'.format(i+1))
    d.append(3*i+1)
    d.append(3*i+2)

dfs = de.drop(de.columns[d],axis=1) #dataframe containing the total shear strain

dfs.columns = strainname #naming the columns something

# dfs.head(10)
```

5 Determining the Elastic Contribution to the Plastic Shear

[ ]:
```
G = 1.429e+09
```

[ ]:
```
stress = np.genfromtxt(filenamestress)
de = pd.DataFrame(stress)

dfstress = de.drop(de.columns[d],axis=1) #Once again used to drop unwanted␣
 ↪columns
dfstress.columns = stressname #naming the columns something

dfel = dfstress.drop(dfstress.columns[0],axis=1)
```

```
del dfstress

dfel = dfel.div(G) #dataframe containing the elastic contributions
dfel.columns = elasticstrainname
```

6 Calculating the Plastic Part of the Shear Strain

[ ]:
```
# need to compute dfs - dfel

def subtraction (df1, df2):
    names = []
    dfnew = df1[[df1.columns[0]]].copy() # first column is copied

    for i in range(len(df1.columns)-1): #refers to the columns
        p =[]
        names.append('Plastic_Strain_{}'.format(i+1))

        for k in range(len(df2)): #refers to the rows
            c = df1.iloc[k,i+1]-df2.iloc[k,i]
            p.append(c)


        dfnew[names[i]] = p

    return(dfnew,names)

a = subtraction(dfs,dfel)

plastic_strainnames = a[1]
dfpl = a[0] #dataframe containing the plastic shear strain contributions

# dfpl.head(10)
```

7 Calculating the Shear Strain Rate

[ ]:
```
def ratecalculator (df):
    ratenames = []
    dfnew = df[[df.columns[0]]].copy() #this makes sure that the first column is␣
 ↪kept in the dataframe, in this case 'Time'

    for i in range(len(df.columns)-1): #refers to the columns
        p = []

        for k in range(len(df)-1): #refers to the rows
```

```
            if k == 0:
                p.append(0)
            else:
                p.append(df.iloc[k+1,i+1]-df.iloc[k-1,i+1]/(df.iloc[k+1,0]-df.
 ↪iloc[k-1,0])) #check this formula

        p.append(0)
        ratenames.append('Strain_Rate_{}'.format(i+1))
        dfnew[ratenames[i]] = p

    return(dfnew,ratenames)
```

[ ]:
```
data = ratecalculator(dfpl)
dataframestrain = data[0]
strainratename = data[1]

del data

# dataframestrain.head(10)
```

8 Pressure File Manipulation

[ ]:
```
trial = pd.read_csv(filenamepressure, names = ['column'], header = None,␣
 ↪usecols=[0])

lenfile = len(trial) #Length of the full pressure file
nrsteps = len(dataframestrain.Time)
```

[ ]:
```
d = [] #empty list, later used to drop columns not containing information

for i in range(lenfile): #This loops to find the regular interval to drop empty␣
 ↪rows from the input file
    if i % (nrsteps+1) == 0:
        d.append(i)

stress = pd.read_csv(filenamepressure, names = ['First'], header = None,␣
 ↪skiprows=d, usecols=[0]) #importing the data
stress[['A', 'Pressure']] = stress.First.str.rsplit(' ', 1, expand=True)␣
 ↪#splitting the column

data = stress.Pressure.to_numpy() #creating an array

a = int(len(data)/len(d)) #Fulle data length divided by the number of empy rows␣
 ↪> number of contributions per element.
stressname = []
```

```
for i in range(len(d)):
    p = int(i*a)
    q = int(i*a + a)
    stressname.append('Pressure{}'.format(i+1))
    if i == 0:
        dataframestress = pd.DataFrame(data[p:q].astype(float), columns =␣
 ↪[stressname[0]])
    else:
        dataframestress[stressname[i]] = data[p:q].astype(float)

# dataframestress.head(10)
```

9 Constants

[ ]:
```
n = 0.447 # 3.1 Criterion building
cstar = 4.867 * (10 ** 4) #3.2 Threshold Value, lower bound in table 3
```

10 Evaluating the Function

[ ]:
```
if len(strainname)-1 == len(stressname):
    df = pd.concat([dataframestrain, dataframestress], axis=1)
else:
    print('There are different numbers of elements in the two datasets')
    print(nope) # this is an intentional error, this means the 'Restart and Run␣
 ↪all'-command is interupted at this cell
```

[ ]:
```
def Valuecalculator (tau, p, gamma_pl, n, cstar): #with tau as the current time,␣
 ↪p as the hydrostatic stress and gamma_pl as the strain rate
    value = []
    exp = float(2 * n / 3)

    for t in range(len(tau)): #determines when the first contribution to the␣
 ↪value occurs
        if p[t] != 0:
            break

    for i in range(len(tau)):
        if p[i] <= 0:
            value.append(0)
        elif tau[i] == tau[t]: #to prevent a division by zero
            value.append(0)
        else:
            value.append((1/cstar) * ((tau[i]-tau[t]) ** (-n)) * p[i] ** (exp) *␣
 ↪abs(gamma_pl[i]))
```

```
    return value
```

[ ]:
```
Dataframe = df[['Time']].copy()
time = Dataframe['Time']

a = elementnr #number of elements, better ways to do this?

valuename = []

for i in range(a): #This loop calls upon the Valuecalculator function per entry␣
 ↪in the dataframes for stress and strain.
    pressure = df[stressname[i]]
    strainrate = df[strainratename[i]]
    value = Valuecalculator(time, pressure, strainrate, n, cstar)
    valuename.append('Value{}'.format(1+i))
    Dataframe[valuename[i]] = value #adding the entry to the new Dataframe where␣
 ↪each entry is the contribution of that time step from the Reaction Criterion
```

11 Trapezoid

[ ]:
```
def trapezoid (t,x):
    c = [0]
    time = t[1]
    for i in range((len(x))-1):
        x1 = x[i]
        x2 = x[i+1]
        b = time * (x1 + x2)  / 2 #This means the time step should be constant
        c.append(b)
    d = np.cumsum(c)
    return c, d
```

[ ]:
```
time = df['Time']
IntValue = df[['Time']].copy()
ReactCrit = df[['Time']].copy()
reacted = []
reacttime = []

for i in range(a): #a still being the number of elements
    datainput = Dataframe[valuename[i]]
    value = trapezoid(time, datainput)
    ReactCrit['ReaCrit_{}'.format(element_list[i])] = value[1]
    for j in range(len(value[1])):
        if value[1][j] >= 1:
            reacted.append(element_list[i])
            reacttime.append(j)
            break
```

```
    IntValue['Intval_{}'.format(element_list[i])] = value[0]

# ReactCrit.head(10)
```

12 Integral Value

[ ]:
```
IntValue.to_excel('Integral value data.xlsx')
```

13 Reaction Criterion

[ ]:
```
ReactCrit.to_excel(newname)
```

14 Reacted Elements Output

[ ]:
```
# print(reacted)
# print(len(reacted))

file = open("Reacted.txt", "w+")

content = str(reacted)
file.write(content)
file.close()

file.close()
```

[ ]:
```
# print(reacttime)
stepnr = min(reacttime)
# print(stepnr)
# print(df['Time'][min(reacttime)])
```

[ ]:
```
fastestelements = []
for i in range(len(reacttime)):
    if reacttime[i] == stepnr:
        fastestelements.append(reacted[i])

# print(fastestelements)
# print(len(fastestelements))
```

B Keyword File Baseline Model

Adapted keyword file. - - - - denotes excluded data.

```
$# LS-DYNA Keyword file created by LS-PrePost(R) V4.8.13 - 20Mar2021
$# Created on Dec-22-2021 (10:21:03)
*KEYWORD
*TITLE
$#                                                                         title
LS-DYNA keyword deck by LS-PrePost
*CONTROL_TERMINATION
$#  endtim    endcyc     dtmin    endeng    endmas     nosol
5.00000E-4         0       0.0       0.01.000000E8         0
*CONTROL_TIMESTEP
$#  dtinit    tssfac      isdo    tslimt     dt2ms      lctm     erode     ms1st
       0.0       0.6         0       0.0       0.0         0         0         0
$#  dt2msf   dt2mslc     imscl    unused    unused     rmscl    unused      ihdo
       0.0         0         0                           0.0                   0
*DATABASE_ELOUT
$#      dt    binary      lcur     ioopt   option1   option2   option3   option4
1.00000E-5         3         0         1         0         0         0         0
*DATABASE_BINARY_D3PLOT
$#      dt      lcdt      beam     npltc    psetid
1.00000E-5         0         0         0         0
$#   ioopt      rate    cutoff    window      type      pset
         0       0.0       0.0       0.0         0         0
*DATABASE_EXTENT_BINARY
$#   neiph     neips    maxint    strflg    sigflg    epsflg    rltflg    engflg
         0         0         3         1         1         1         1         1
$#  cmpflg    ieverp    beamip     dcomp      shge     stssz    n3thdt   ialemat
         0         0         0         1         1         1         2         1
$# nintsld   pkp_sen      sclp     hydro     msscl     therm    intout    nodout
         0         0       1.0         0         0         0
$#    dtdt    resplt     neipb     quadr     cubic
         0         0         0         0         0
*DATABASE_HISTORY_SHELL_SET
$#     id1       id2       id3       id4       id5       id6       id7       id8
         1         0         0         0         0         0         0         0
*BOUNDARY_SPC_SET
$#    nsid       cid      dofx      dofy      dofz     dofrx     dofry     dofrz
         3         0         1         1         1         1         1         1
*SET_NODE_LIST_TITLE

    ----

*BOUNDARY_SPC_SET
$#    nsid       cid      dofx      dofy      dofz     dofrx     dofry     dofrz
         5         0         1         0         1         1         1         1
*SET_NODE_LIST_TITLE
NODESET(SPC) 5

    ----

*CONTACT_2D_AUTOMATIC_SINGLE_SURFACE_TITLE
```

```
$#     cid                                                          title
         1Contact
$#    sids      sidm     sfact      freq        fs        fd        dc     membs
         1         1       1.0        50       0.0       0.0       0.0         6
$#  tbirth    tdeath       sos       som       nds       ndm       cof      init
       0.01.00000E20       1.0       1.0         0         0         0         0
$#      vc       vdc       ipf     slide    istiff   tiedgap    igapcl    tietyp
       0.0      10.0         0         0         0       0.0         0         0
$#  sldsos    sldsom     tdpen
       0.0       0.0       0.0
*SET_PART_LIST_TITLE
Projectileset
$#     sid       da1       da2       da3       da4    solver
         1       0.0       0.0       0.0       0.0MECH
$#    pid1      pid2      pid3      pid4      pid5      pid6      pid7      pid8
         1         3         4         0         0         0         0         0
*PART
$#                                                               title
Projectile
$#     pid     secid       mid     eosid      hgid      grav    adpopt      tmid
         1         1         1         0         0         0         0         0
*SECTION_SHELL_TITLE
Shell section
$#   secid    elform      shrf       nip     propt   qr/irid     icomp     setyp
         1        14     0.833         2       1.0         0         0         1
$#      t1        t2        t3        t4      nloc     marea      idof    edgset
       0.0       0.0       0.0       0.0       0.0       0.0       0.0         0
*MAT_PLASTIC_KINEMATIC_TITLE
Steel
$#     mid        ro         e        pr      sigy      etan      beta
         1    7850.02.10000E11       0.34.000000E8       0.0       1.0
$#     src       srp        fs        vp
       0.0       0.0       0.0       0.0
*PART
$#                                                               title
Energetic Material
$#     pid     secid       mid     eosid      hgid      grav    adpopt      tmid
         3         1         2         0         0         0         0         0
*MAT_DRUCKER_PRAGER_TITLE
Energetic material
$#     mid        ro      gmod       rnu       rkf       phi      cval       psi
         2    1800.01.429000E9       0.4       1.0  0.349066   1750520 0.0174533
$# str_lim
     0.005
$#  gmoddp     phidp    cvaldp     psidp    gmodgr     phigr    cvalgr     psigr
       0.0       0.0       0.0       0.0       0.0       0.0       0.0       0.0
*PART
$#                                                               title
Steel test-set-up
$#     pid     secid       mid     eosid      hgid      grav    adpopt      tmid
         4         1         1         0         0         0         0         0
*MAT_ELASTIC_TITLE
Dummy elastic
$#     mid        ro         e        pr        da        db  not used
```

```
         3    1800.04.000000E9       0.4       0.0       0.0       0.0
*INITIAL_VELOCITY_GENERATION
$#      id      styp     omega        vx        vy        vz     ivatn      icid
         1         2       0.0       0.0     -77.0       0.0         0         0
$#      xc        yc        zc        nx        ny        nz     phase    irigid
       0.0       0.0       0.0       0.0       0.0       0.0         0         0
*ELEMENT_SHELL

    ----

*NODE

    ----

*SET_NODE_LIST_TITLE
NODESET(SPC) 4

    ----

*SET_SHELL_LIST

    ----

*END
```